Albendazole reduces endoplasmic reticulum stress induced by *Echinococcus multilocularis* in mice

Running title: ER-stress induced by *E. multilocularis*

Michael Weingartner[1#], Fadi Jebbawi[1#], Junhua Wang[2,3], Simon Stücheli[1], Bruno Gottstein[2,3], Guido Beldi[4], Britta Lundström-Stadelmann[2], and Alex Odermatt[1*]

[1] Division of Molecular and Systems Toxicology, Department of Pharmaceutical Sciences, University of Basel, Basel, Switzerland.

[2] Institute of Parasitology, Department of Infectious Diseases and Pathobiology, Vetsuisse Faculty, University of Bern, Bern, Switzerland.

[3] Institute for Infectious Diseases, Faculty of Medicine, University of Berne, Berne, Switzerland.

[4] Department of Visceral Surgery and Medicine, University Hospital of Berne, Berne, Switzerland.

* To whom correspondence should be addressed:
Dr. Alex Odermatt, Division of Molecular and Systems Toxicology, Department of Pharmaceutical Sciences, University of Basel, Klingelbergstrasse 50, 4056 Basel, Switzerland
Email: alex.odermatt@unibas.ch

[#]These authors contributed equally to the presented study

Disclosures: The authors declare no commercial or financial conflict of interest

Keywords: Alveolar echinococcosis; benzimidazole; endoplasmic reticulum; unfolded protein response; parasite; inflammation; infection; microRNA

Abstract

Background

Echinococcus multilocularis causes alveolar echinococcosis (AE), a rising zoonotic disease in the northern hemisphere. Treatment of this fatal disease is limited to chemotherapy using benzimidazoles and surgical intervention, with relatively frequent disease recurrence in cases without radical surgery. Elucidating the molecular mechanisms underlying *E. multilocularis* infections and host-parasite interactions aids developing novel therapeutic options. This study explored an involvement of unfolded protein response (UPR) and endoplasmic reticulum-stress (ERS) during *E. multilocularis* infection in mice.

Methods

E. multilocularis- and mock-infected C57BL/6 mice were subdivided six weeks after infection into vehicle and albendazole (ABZ) treated groups. Eight weeks later, liver tissue was collected to examine mRNA, microRNA (miR) and protein expression of UPR- and ERS-related genes.

Results

E. multilocularis infection upregulated UPR- and ERS-related proteins, including ATF6, CHOP, GRP78, ERP72, H6PD and calreticulin, whilst PERK and its target eIF2α were not affected, and IRE1α and ATF4 were downregulated. ABZ treatment in *E. multilocularis* infected mice reversed the increased ATF6 and calreticulin protein expression, tended to reverse increased CHOP, GRP78, ERP72 and H6PD expression, and decreased ATF4 and IRE1α expression to levels seen in mock-infected mice. The expression of miR-146a-5p (downregulated by IRE1α) and miR-1839-5p (exhibiting a unique target site in the IRE1α 3'UTR) were significantly increased in *E. multilocularis* infected mice, an effect reversed by ABZ treatment. Other miRs analyzed were not altered in *E. multilocularis* infected mice.

Conclusions and Significance

AE causes UPR activation and ERS in mice. The *E. multilocularis*-induced ERS was ameliorated by ABZ treatment, indicating its effectiveness to inhibit parasite proliferation and downregulate its activity status. ABZ itself did not affect UPR in control mice. Identified miR-146a-5p and miR-1839-5p might represent biomarkers of *E. multilocularis* infection. Modulation of UPR and ERS, in addition to ABZ administration, could be exploited to treat *E. multilocularis* infection.

Author summary

Alveolar echinococcosis is a zoonotic disease caused by the fox tapeworm *Echinococcus multilocularis*. Treatment of this fatal disease is limited to surgical intervention, preferably radical curative surgery if possible, and the use of parasitostatic benzimidazoles. It is not yet fully understood how the parasite can remain in the host's tissue for prolonged periods, complicating the development of therapeutic applications. This work investigated an involvement of the unfolded protein response (UPR) and endoplasmic reticulum-stress (ERS) during *E. multilocularis* infection and upon treatment with albendazole (ABZ) in mice. The results revealed increased expression levels of the ERS sensor ATF6 and of downstream target genes in liver tissue of *E. multilocularis*- compared to mock-infected mice. Additionally, H6PD, generating NADPH within the endoplasmic reticulum, and the lectin-chaperone calreticulin were increased in *E. multilocularis* infected liver tissue while the expression of the ERS associated genes ATF4 and IRE1α were decreased. The miR-1839-5p and miR-146-p, linked to IRE1α, were elevated upon *E. multilocularis* infection, offering potential as novel biomarkers of alveolar echinococcosis. The observed gene expression changes were at least partially reversed by ABZ treatment. Whether modulation of UPR and ERS targets can improve the therapy of alveolar echinococcosis remains to be investigated.

Abbreviations

ABZ, albendazole; AE, alveolar echinococcosis; ATF4, activating transcription factor 4; ATF6, activating transcription factor 6; CHOP, CCAAT/enhancer-binding protein homologous protein; CNX, calnexin; CRT, calreticulin; CTRL, control; *E. multilocularis*, *Echinococcus multilocularis*; GRP78, glucose-binding protein 78; eIF2α, eukaryotic initiation factor 2α; ER, endoplasmic reticulum; ERAD, ER-associated degradation; ERP72, endoplasmic reticulum resident protein 72; ERS, endoplasmic reticulum stress; H6PD, hexose-6-phosphate dehydrogenase; HRP, horse-radish peroxidase; IRE1α, inositol-requiring enzyme 1α; microRNA(s), miR(s); PERK, protein kinase R (PKR) like ER kinase; PVDF, polyvinylidene difluoride; RIPA, radioimmunoprecipitation assay; RT-qPCR, real-time quantitative polymerase chain reaction; UPR, unfolded protein response; XBP1(-s), X-box binding protein 1 (-spliced);

Introduction

Alveolar echinococcosis (AE) is a severe helminthic disease caused by accidental ingestion of eggs from the fox tapeworm *Echinococcus multilocularis (E. multilocularis)* [1, 2]. After an incubation period of 5 up to 15 years without perceivable symptoms, AE has a fatal outcome in up to 90% of cases when left untreated [3-5]. AE is characterized by a slow but progressive tumor-like growth of metacestodes (larval stage) mainly in the liver, with a tendency to spread to various organs like spleen, brain, heart and other tissues such as bile ducts and blood vessels [6-8]. Treatment by radical surgical resection is limited by the diffuse infiltrations of AE lesions in liver and other tissues in advanced cases [9, 10]. If lesions cannot be completely removed by surgery, a lifelong medication is required, usually using benzimidazoles, which can cause adverse side effects. For example, several cases with hepatotoxic effects due to treatment with

the benzimidazole albendazole (ABZ) were reported with various outcomes [11-14]. An inadequate adherence to chemotherapy, due to adverse side effects, can explain the relapsing spread of AE and a worsening general condition of patients with severe *E. multilocularis* infiltrations [15, 16]. Considering these circumstances, the rising numbers of reported cases of AE especially in Europe and the lack of a curative drug treatment, emphasizes the necessity to further investigate the mechanisms underlying this threat and search for improved therapeutic options [17-22].

Several bacteria and viruses have been described to modulate endoplasmic reticulum (ER) stress (ERS) and unfolded protein response (UPR), either by bacterial virulence factors such as toxins (e.g. cholera toxin, pore-forming toxins) or by the increased demand of newly synthesized proteins for the production of virions [23-28]. Activation of the UPR via an induction of glucose-regulated protein 78 (GRP78) has previously been shown in cells infected with *Human immunodeficiency virus* (HIV) [27, 29], *Dengue virus* (DENV) [30], *West Nile virus* (WNV) [31] or *Human cytomegalovirus* (HCMV) [32]. Moreover, facilitated replication of viruses and immune evasion represent key features following UPR activation by *Mouse hepatitis virus* (MHV) [33] and *Herpes simplex virus 1* (HSV-1) [34]. On the other hand, an ERS-induced upregulation of UPR-related genes was linked to an enhanced production of pro-inflammatory cytokines in B-cells and stellate cells [35, 36]. A modulation of the UPR pathway was reported not only during viral but also bacterial infections. *Legionella pneumophila* infection led to an inhibition of X-box binding protein 1 (XBP1) splicing in mammalian host cells, thereby suppressing the host UPR pathway [37]. *Mycobacterium tuberculosis* was found to induce ERS, indicated by increased CCAAT/enhancer-binding protein homologous protein (CHOP) and GRP78 protein levels in infected macrophages, leading to host cell apoptosis. Decreased levels of phosphorylated eukaryotic initiation factor 2α (eIF2α) in infected cells were associated with enhanced bacterial survival [38].

However, to date the knowledge of pathogen-induced ERS and UPR activation is incomplete and mainly limited to bacterial and viral infections. In this regard, a modulation of the host's UPR with an upregulation of CHOP was observed in *Toxoplasma gondii* infected cells, leading to apoptosis of host cells [39]. Another study in a mouse model provided evidence that *Plasmodium berghei* exploits the host's UPR machinery for its survival [40]. However, little is known about the involvement of ERS and UPR activation in *E. multilocularis* infection.

The present study addressed a possible role of the modulation of UPR- and ERS-related proteins in host cells in response to AE and investigated the effect of these pathways using *E. multilocularis* infected mice as a model. A better understanding of a contribution of proteins of the UPR and ERS pathways in the context of infectious diseases is of interest regarding the development of improved therapeutic strategies to cope with parasitic infections [41-43].

Additionally, this work investigated whether microRNAs (miRs), small non-coding single stranded RNAs (17-24 nucleotides) that regulate the post-transcriptional levels of mRNAs by inhibiting their translation to proteins, may be altered upon *E. multilocularis* infection. Several studies revealed a functional interaction between UPR/ERS signaling and the expression of miRs [44-46]. Silencing of miRs was found to be involved in ERS signaling and miRs act as effectors and modulators of the UPR and ERS pathways [47]. The miRs, isolated from human specimen, including urine, saliva, serum and tissues, are considered as biomarkers of several immune pathologies such as cancer, autoimmune diseases and viral or bacterial infections [48-54]. In this regard, recent investigations provided evidence for a role of some miRs in the regulation of UPR signaling, with miR-181a-5p and miR-199a-5p shown to suppress the UPR master regulator GRP78 [47, 55, 56]. On the other side, UPR pathways also can affect the expression of some miRs, as shown by inositol-requiring enzyme 1α (IRE1α) that cleaves the precursors of anti-apoptotic miR-17-5p, miR-34a-5p, miR-96-5p and mir-125b-5p, which in turn negatively regulate the expression of caspase 2 and thioredoxin-interacting protein [57, 58]. In addition, the activation of protein kinase R (PKR)-like ER kinase (PERK) induces the

157 expression of miR-30c-2-3p, which downregulates XBP1, representing a possible negative
158 crosstalk between PERK and IRE1α [58].
159 Boubaker et al. recently described a murine miR signature in response to early stage *E.*
160 *multilocularis* egg infection where the expression of seven miRs (miR-148a-3p, miR-143-3p,
161 miR-101b-3p, miR-340-5p, miR-22-3p, miR-152-3p and miR-30a-5p) was decreased in AE-
162 infected compared to mock-infected mice. In contrast, *E. multilocularis* infected mice exhibited
163 significantly higher levels of miR-21a-5p, miR-28a-5p, miR-122-5p and miR-1839-5p
164 compared to the mock-infected controls [59]. The miRs mentioned above were therefore also
165 analyzed in the present study.
166

167 # Materials and Methods

168 ## Chemicals and reagents

169 Polyvinylidene difluoride (PVDF) membranes (Cat# IPVH00010, pore size: 0.45 µm),
170 Immobilon Western Chemiluminescence horseradish-peroxidase (HRP) substrate kit,
171 radioimmunoprecipitation assay (RIPA) buffer, β-mercaptoethanol, HRP-conjugated goat anti-
172 mouse secondary antibody (Cat# A0168, RRID:AB_257867), rabbit polyclonal anti-hexose-6-
173 phosphate dehydrogenase (H6PD) antibody (Cat# HPA004824, RRID:AB_1079037), protease
174 inhibitor cocktail, dNTPs, KAPA SYBR® FAST kit and qPCR kit were purchased from Merck
175 (Darmstadt, Germany). RNeasy Mini kit and QIAcube were obtained from Qiagen (Venlo,
176 Netherlands), GoScript reverse transcriptase (Cat# A5003) from Promega (Fitchburg, WI,
177 USA), rabbit monoclonal anti-lamin B1 antibody (Cat# ab133741, RRID:AB_2616597) from
178 Abcam (Cabridge, UK) and mouse monoclonal anti-GRP78 antibody (Cat# 610978,
179 RRID:AB_398291) from BD Bioscience (Franklin Lakes, NJ, USA). HRP-conjugated goat
180 anti-rabbit secondary antibody (Cat# 7074, RRID:AB_2099233), mouse monoclonal anti-
181 CHOP antibody (Cat# 2895, RRID:AB_2089254), rabbit polyclonal anti-calreticulin (CRT)
182 antibody (Cat# 2891, RRID:AB_2275208), rabbit polyclonal anti-eIF2α antibody (Cat# 9722,

RRID:AB_2230924), rabbit monoclonal anti-ATF4 antibody (Cat# 11815, RRID:AB_2616025) and rabbit monoclonal anti-ATF6 antibody (Cat# 65880, RRID:AB_2799696) were purchased from Cell Signaling (Cambridge, UK). Mouse monoclonal anti-PERK antibody (Cat# sc-377400, RRID:AB_2762850), anti-IRE1α antibody (Cat# sc-390960, RRID: N/A) and anti-ERp72 antibody (Cat# sc-390530, RRID: N/A) were obtained from Santa Cruz Biotechnology (Dallas, TX, USA). Pierce® bicinchoninic acid protein assay kit, Nanodrop™ One C (Cat# 13-400-519) and Trizol® total RNA isolation reagent were purchased from Thermo Fisher Scientific (Waltham, MA, USA). Precellys-24 tissue homogenizer was purchased from Bertin Instruments (Montigny-le-Bretonneux, France). Primers for real-time quantitative polymerase chain reaction (RT-qPCR) were obtained from Microsynth (Balgach, Switzerland). TaqMan microRNA Assays, snoRNA234, TaqMan microRNA reverse transcription kit (Cat# 4366596), TaqMan fast advanced master mix (Cat# 4444556), TaqMan probes (Cat# 4427975, Assay IDs 000468, 000389, 000398, 000470, 121135_mat, 000416, and 001234) and ViiA 7 real-time PCR system (Cat# 4453545) were purchased from Applied Biosystems (Foster City, CA, USA). Rabbit polyclonal anti-calnexin (CNX) antibody (Cat# SAB4503258, RRID:AB_10746486) and all other reagents were purchased from Sigma-Aldrich (St. Louis, MO, USA).

Ethics Statement

The animal studies were performed in compliance with the recommendations of the Swiss Guidelines for the Care and Use of Laboratory Animals. The protocol used for this work was approved by the governmental Commission for Animal Experimentation of the Canton of Bern (approval no. BE112/17).

Animal experimentation and sampling

208 Animal experimentation, liver tissue extraction and corresponding liver tissue samples were
209 previously described by Wang et al. [60]. Briefly, female 8-week-old wild type C57BL/6 mice
210 were randomly distributed into 4 groups with 6 animals per group: 1) mock-infected (corn oil
211 treated) control mice (referred to as "CTRL"); 2) *E. multilocularis* infected, vehicle treated mice
212 (referred to as "AE"); 3) *E. multilocularis* infected, ABZ-treated mice (referred to as "AE-
213 ABZ"); and 4) mock-infected, ABZ-treated mice (referred to as "ABZ") (S1 Fig). All animals
214 were housed under standard conditions in a conventional daylight/night cycle room with access
215 to feed and water *ad libitum* and in accordance with the Federation of European Laboratory
216 Animal Science Association (FELASA) guidelines. During the experimental period animals
217 were examined weekly for subjective presence of health status and changes in weight. At the
218 end of the experiment the mice were euthanized by CO_2 and liver tissue was resected followed
219 by immediate freezing in liquid nitrogen and storage at -80°C until use.
220
221 **Parasite preparation and secondary infection of mice by intraperitoneal administration**
222 Infection with *E. multilocularis* by intraperitoneal injection was conducted as previously
223 described [61]. Briefly, *E. multilocularis* (isolate H95) was extracted and maintained by serial
224 passages in C57BL/6-mice. Aseptic removal of infectious material from the abdominal cavity
225 of infected animals was used for continuation of AE in mice. Collected tissue was grinded
226 through a sterile 50 µm sieve, roughly 100 vesicular cysts were suspended in 100 µL sterile
227 PBS and administrated *via* intraperitoneal injection to group 2 ("AE") and 3 ("AE-ABZ"). Mice
228 of the mock-infected groups 1 ("CTRL") and 4 ("ABZ") received 100 µL of sterile PBS.
229
230 **Treatment**
231 Treatment started 6 weeks after initial infection (S1 Fig). 100 µL corn oil were orally
232 administrated to groups 1 ("CTRL") and 2 ("AE") five times per week. Group 3 ("AE-ABZ")

and 4 ("ABZ") received 100 µL corn oil containing ABZ (200 mg/kg body weight) orally five times per week. The treatment was terminated after 8 weeks and mice were euthanized.

Analysis of protein expression by western blot

The procedures for liver sample preparation and western blot analysis have been previously described [62]. Briefly, liver samples (approximately 7 mg) were homogenized (30s, 6500 rpm, at 4°C, using a Precellys-24 tissue homogenizer) in 450 µL RIPA buffer (50 mM Tris-HCl, pH 8.0, with 150 mM NaCl, 1.0% NP-40, 0.5% sodium deoxycholate and 0.1% sodium dodecyl sulfate) containing protease inhibitor cocktail and centrifuged (4 min, 16,000 × g, 4°C). Protein concentration was measured by a standard bicinchoninic acid assay (Pierce® BCA Protein Assay Kit). Samples were boiled (5 min at 95°C) in Laemmli solubilization buffer (60 mM Tris-HCl, 10% glycerol, 0.01% bromophenol blue, 2% sodium dodecyl sulfate, pH 6.8, 5% β-mercaptoethanol). The protein extract (20 µg) was separated by 10-14% SDS-PAGE and blotted on PVDF membranes. The membranes were blocked (1 h, room temperature) in TBST-BSA, (20 mM Tris buffered saline with 0.1% Tween-20, 1% bovine serum albumin). All primary and secondary antibody dilutions and incubations were performed in TBST-BSA. For the detection of primary antibodies raised in rabbit, secondary HRP-conjugated goat anti-rabbit antibody was used. Primary antibodies raised in mouse were detected by HRP-conjugated goat anti-mouse antibody. Primary antibodies were incubated at 4°C over-night. Secondary antibodies were applied at room temperature for 1 h. Protein content was visualized by Immobilon Western Chemiluminescence HRP substrate. Protein bands were quantified by densitometry normalized to Lamin B1 protein levels using ImageJ software (version 1.53n). The applications of primary and secondary antibodies can be found in S1 Table.

Quantification of mRNA by RT-qPCR

Methods for preparation of liver samples, RNA isolation and RT-qPCR analysis were performed as described [60]. Briefly, total RNA was isolated from liver tissue (approximately 8 mg) by homogenization (30 s, 6500 rpm, 4°C; Precellys-24 tissue homogenizer) in 350 µL RLT buffer (RNeasy Mini Kit) supplied with 40 mM dithiothreitol, followed by centrifugation (3 min, 16,000 × g). The supernatant was further processed according to the manufacturer's protocol for RNA isolation from animal tissues and cells using QIAcube. RNA quality and concentration was analyzed using Nanodrop™ One C. 1000 ng of RNA was transcribed into cDNA using GoScript Reverse Transcriptase. KAPA SYBR® FAST Kit was used for RT-qPCR (4 ng of cDNA per reaction in triplicates, 40 cycles) analysis, and reactions were performed using a Rotor Gene Real-Time Cycler (Corbett Research, Sydney, New South Wales, Australia). Data was normalized to the expression levels of the endogenous control gene β-actin. Comparison of gene expression was performed using the 2-ΔCT-method using β-actin as housekeeping gene [63]. Primers used for RT-qPCR are listed in S2 Table.

Extraction and quantification of miRNA by qPCR

Total RNA was extracted from liver tissues using Trizol® total RNA isolation reagent and RNA concentration quantified using Nanodrop™ One C. TaqMan microRNA assays were used to quantify mature miR expression. SnoRNA234 was used as endogenous control of miR expression. Thus, miR-specific reverse transcription was performed for each miR using 10 ng of purified total RNA, 100 mM dNTPs, 50 U multiple reverse transcriptase, 20 U RNase inhibitor, and 50 nM of miR-specific reverse transcription primer samples using the TaqMan MicroRNA Reverse Transcription kit. Reactions with a volume of 15 µL were incubated for 30 min at 16°C, 30 min at 42°C, and 5 min at 85°C to inactivate the reverse transcriptase. RT-qPCR (5 µL of reverse transcription product, 10 µL TaqMan Fast Advanced Master Mix and 1 µL TaqMan microRNA Assay Mix containing PCR primers and TaqMan probes) were run in triplicates at 95°C for 10 min followed by 40 cycles at 95°C for 15 s and 60°C for 1 min.

Quantitative miR expression data were acquired and analyzed using the ViiA 7 real-time PCR system (Applied Biosystems, Cat# 4453545).

Statistical analyses

Data are presented as mean ± SD. The significance of the differences between the examined animals were determined by Kruskal-Wallis test or one-way ANOVA, whereby the specific test is indicated in the Figure legend. No outliers were excluded. *P≤0.05; **P≤0.01; ***P≤0.001 significantly different as indicated. GaphPad Prism software (version 8.0.2, GraphPad, La Jolla, CA, USA) was used for statistical analysis.

Results

Effects of AE on the expression of proteins related to UPR and ERS pathways

As the present knowledge on the modulation of UPR and ERS pathways during parasitic infections is limited, this study examined the expression of key proteins related to these pathways in liver tissues of mice infected with *E. multilocularis*. In the applied model of secondary *E. multilocularis* infection, differential effects on the expression of proteins of the different UPR and ERS branches were observed. Among the PERK pathway, ATF4 protein levels were significantly decreased in liver tissue of AE mice compared to mock-infected controls (Table 1, Fig 1). The expression of PERK and its target protein eIF2α were not affected by *E. multilocularis* infection. However, the most pronounced effects were observed for ERS related proteins of the ATF6 branch of the UPR (Table 1, Fig 2). The levels of all four proteins analyzed were elevated, whereby the luminal chaperone and protein disulfide isomerase ERP72 and the ERS marker CHOP were 2.0-fold and 4.5-fold increased and ATF6 and GRP78 tended to be elevated with 2.2-fold and 2.7-fold higher levels, respectively. IRE1α protein expression was decreased by about 3-fold in *E. multilocularis* infected compared to control mouse liver tissues (Table 1, Fig 3), whilst its target the spliced form of XBP1 showed a trend to lower

310 levels in liver tissues of infected mice (S2 Fig). However, XBP1 protein expression could not
311 be assessed as no specific antibody could be identified.
312
313 **Table 1. Expression of proteins involved in UPR and ERS pathways.** Protein levels in liver
314 tissue samples were analyzed by western blot and densitometry (animals per group n=6).
315 Numbers represent protein expression levels normalized to those of the control (CTRL) group
316 (mean ± SD). Significantly decreased protein levels are highlighted in red and increased protein
317 levels in blue. Symbols indicate significant differences ($p \leq 0.05$) between groups: *, compared
318 to CTRL; §, compared to ABZ; #, compared to AE-ABZ. No outliers were excluded. Non-
319 parametric, Kruskal-Wallis test.
320
321

		Group			
Classification Pathway	**Relative protein expression** (normalized to CTRL)	**CTRL** (n=6)	**AE** (n=6)	**AE-ABZ** (n=6)	**ABZ** (n=6)
PERK branch	PERK	1.0	1.1 (±0.8)	1.1 (±0.5)	2.8 (±2.6)
	eIF2α	1.0	1.5 (±0.5)	1.6 (±0.4)	1.1 (±0.4)
	ATF4	1.0	0.3 (±0.1)*,§	0.8 (±0.2)	1.0 (±0.4)
ATF6 branch	ATF6	1.0	2.2 (±1.0)$^{\#}$	0.6 (±0.2)	1.2 (±0.5)
	CHOP	1.0	4.5 (±2.0)*,§	3.0 (±1.4)§	1.0 (±0.3)
	GRP78	1.0	2.7 (±1.5)§	1.3 (±1.1)	1.0 (±0.3)
	ERP72	1.0	2.0 (±0.6)*,§	1.3 (±0.6)	0.9 (±0.4)
IRE1 branch	IRE1α	1.0	0.3 (±0.2)*,§	0.8 (±0.4)	1.3 (±0.7)
ER chaperones	Calnexin (CNX)	1.0	0.9 (±0.2)	1.2 (±0.6)	1.2 (±0.5)
	Calreticulin (CRT)	1.0	1.6 (±0.5)$^{\#,§}$	0.9 (±0.3)	0.8 (±0.3)
NADPH generation	H6PD	1.0	2.6 (±1.8)*	1.4 (±0.6)	1.4 (±0.6)

322

Fig 1. *E. multilocularis* infection decreases ATF4 protein levels. Western blot and semi-quantitative analysis by densitometry of protein levels of PERK, eIF2α and ATF4 in mock-infected control mice (CTRL), *E. multilocularis* infected mice (AE), infected mice treated with ABZ (AE-ABZ) or uninfected mice treated with ABZ (ABZ). One representative blot (of two) containing samples from three different mice is shown in the top panel. Densitometry results represent data from the two blots on samples from six mice (mean ± SD), normalized to lamin B1 control and with CTRL set as 1. No outliers were excluded. The non-parametric Kruskal-Wallis test was used to assess significance. *P≤0.05; ***p≤ 0.001.

Fig 2. Induction of the ATF6-branch of the UPR by *E. multilocularis* infection. Western blot and semi-quantitative analysis by densitometry of the protein levels of ATF6, CHOP, GRP78 and ERP72 in mock-infected control mice (CTRL), *E. multilocularis* infected mice (AE), infected mice treated with ABZ (AE-ABZ) or uninfected mice treated with ABZ (ABZ). One representative blot (of two) containing samples from three different mice is shown in the top panel. Densitometry results represent data from the two blots on samples from six mice (mean ± SD), normalized to lamin B1 control and with CTRL set as 1. No outliers were excluded. The non-parametric Kruskal-Wallis test was used to assess significance. *P≤0.05; **p≤0.01; ***p≤ 0.001.

Fig 3. Decreased IRE1α protein expression upon *E. multilocularis* infection. Western blot and semi-quantitative analysis by densitometry of IRE1α protein levels in mock-infected control mice (CTRL), *E. multilocularis* infected mice (AE), infected mice treated with ABZ (AE-ABZ) or uninfected mice treated with ABZ (ABZ). One representative blot (of two) containing samples from three different mice is shown in the top panel. Densitometry results represent data from the two blots on samples from six mice (mean ± SD), normalized to lamin B1 control and with CTRL set as 1. No outliers were excluded. The non-parametric Kruskal-Wallis test was used to assess significance. *P≤0.05; **p≤0.01.

Additional proteins with a role in ER-redox regulation and ERS include the ER resident lectin chaperones CNX and CRT. Whilst CNX protein levels were unaffected by *E. multilocularis* infection, CRT protein expression was significantly increased in AE mice compared to controls (Table 1, Fig 4). Additionally, the expression levels of the luminal NADPH-generating enzyme H6PD were determined, revealing a 2.6-fold higher expression in AE compared to control mice (Table 1, Fig 5).

Fig 4. The expression of the luminal chaperone CRT is increased upon *E. multilocularis* infection and reversed by ABZ treatment. Western blot and semi-quantitative analysis by densitometry of CNX and CRT protein levels in mock-infected control mice (CTRL), *E. multilocularis* infected mice (AE), infected mice treated with ABZ (AE-ABZ) or uninfected mice treated with ABZ (ABZ). One representative blot (of two) containing samples from three different mice is shown in the top panel. Densitometry results represent data from the two blots on samples from six mice (mean ± SD), normalized to lamin B1 control and with CTRL set as 1. No outliers were excluded. The non-parametric Kruskal-Wallis test was used to assess significance. *P≤0.05.

Fig 5. Increased H6PD protein expression upon *E. multilocularis* infection. Western blot and semi-quantitative analysis by densitometry of protein levels of H6PD in mock-infected control mice (CTRL), *E. multilocularis* infected mice (AE), infected mice treated with ABZ (AE-ABZ) or uninfected mice treated with ABZ (ABZ). One representative blot (of two) containing samples from three different mice is shown in the top panel. Densitometry results represent data from the two blots on samples from six mice (mean ± SD), normalized to lamin B1 control and with CTRL set as 1. No outliers were excluded. The non-parametric Kruskal-Wallis test was used to assess significance. *P≤0.05.

Treatment with ABZ reverses the effects of AE on proteins involved in UPR and ERS

Treatment of AE mice with ABZ (AE-ABZ group) resulted in a reversal of the *E. multilocularis* induced alterations of UPR and ERS related protein expression (Table 1). Also the effects on the ER chaperones CNX and the NADPH-generating H6PD were reversed by ABZ treatment. An exception was CHOP that was still upregulated in ABZ treated infected mice. Importantly, ABZ did not cause any significant alterations in the expression of the proteins analyzed in uninfected control mice (Table 1, Figs 1-5). Protein levels of PERK show a trend to be increased in ABZ treated, uninfected animals (Fig 1); however, this did not reach significance due to high variance in the detected signals.

Increased miR-146a-5p and miR-1839-5p expression in secondary *E. multilocularis* infection and reversal by ABZ treatment

Boubaker et al. [59], using an early stage mouse model of *E. multilocularis* infection, identified several miRs with altered expression in liver tissues from infected mice. In the present study, the levels of the miRs exhibiting a target site in the 3'UTR of genes involved in UPR and ERS

pathways were determined. The analysis of the seven mouse miRs miR-148a-3p, miR-15a-5p, miR-22, miR-146a-5p, miR-1839-5p, miR-30a-5p and miR-30a-3p revealed significantly higher levels (2.1-fold and 3.2-fold, respectively) of miR-1839-5p and miR-146a-5p in liver tissue samples of *E. multilocularis* infected mice (AE) compared to control animals (CTRL). The other miRs remained unchanged (S3 Fig). Interestingly, ABZ treatment of AE mice decreased miR-1839-5p (2.8 fold) and miR-146a-5p (5.8 fold) compared to the levels found in CTRL animals or even lower, and ABZ alone tended to decrease miR-1839-5p and miR-146a-5p expression levels (Fig 6).

Figure 6

Altered expression of IRE1α related miRs upon *E. multilocularis* infection and reversal by ABZ treatment. A) Nucleotide sequence containing the murine IRE1α mRNA 3'- UTR. The start and stop codon of the IRE1α CDS are indicated in bold and the miR-1839-5p binding site is highlighted by red and bold letters. B) IRE1α mRNA levels normalized to the β-actin housekeeping gene and relative to the levels obtained in control mice, and miR-1839-5p levels normalized to the Sno234 housekeeping gene and relative to uninfected controls. C) miR-146-5p levels normalized to Sno234 and relative to uninfected controls. B, C) mock-infected control mice ($CTRL_{n=6}$), *E. multilocularis* infected mice ($AE_{n=6}$), infected mice treated with ABZ ($AE\text{-}ABZ_{n=6}$) or uninfected mice treated with ABZ ($ABZ_{n=6}$). Results represent mean ± SD. No outliers were excluded. One-way ANOVA test was used to assess significance. *P≤0.05; **p≤0.01; ***p≤ 0.001.

Discussion

Recent studies on viral, bacterial or intracellular parasitic infections emphasize the important roles of the UPR and ERS pathways in pathogen induced diseases [23-25, 64, 65]. Activation

421 of the UPR, a specific form of ERS triggered by an accumulation of unfolded or misfolded
422 proteins within the ER, can be mediated by three branches, represented by the ER
423 transmembrane stress sensor proteins ATF6, PERK and IRE1α [66-74] (Fig 7). In non-stressed
424 cells, these proteins remain in an inactive state, bound to the luminal chaperone GRP78. Upon
425 activation, GRP78 is released to support luminal protein folding, followed by the activation of
426 ATF6, PERK and IRE1α and their downstream targets such as eIF2α, ATF4, XBP1 and CHOP
427 in order to mediate the stress response [75-77].
428
429 **Fig 7. Schematic overview of ERS signaling pathways under basal and *E. multilocularis***
430 **infection stressed conditions.** The ER chaperone GRP78 binds to unfolded luminal proteins
431 and dissociates from the three major ERS sensors: ATF6, IRE1α and PERK. Loss of GRP78
432 binding leads to the translocation of ATF6 to the golgi apparatus, where it is cleaved by
433 proteases. The cleaved form of ATF6 translocates into the nucleus to act as a transcription factor
434 for ER chaperons (*e.g.* ERP72) and ERS related genes. ERS promotes IRE1α dimerization and
435 autophosphorylation, which activates the endoribonuclease activity resulting in the splicing and
436 thereby activation of XBP. XBP1-s promotes the expression of ERAD related genes and
437 chaperones (*e.g.* GRP78). Activation of PERK is initiated by dimerization and self-
438 phosphorylation. Activated PERK phosphorylates eIF2α, leading to eIF2α-mediated inhibition
439 of global protein translation in order to decrease the luminal protein load. Besides,
440 phosphorylated eIF2α increases the transcription of ATF4, which in turn upregulates expression
441 of genes related to cell homeostasis restoration. If prolonged ERS occurs and pro-adaptive UPR
442 fails, ATF4 induces genes (including CHOP) leading to apoptosis. During ERS, increased
443 levels of miR-1839-5p are proposed to control IRE1α gene expression and therefore affect the
444 cellular ERS response.
445
446

447 The results of the present study revealed a pronounced induction of ATF6 in livers of mice
448 infected with *E. multilocularis*. In contrast, the PERK and IRE1α branches were not activated
449 but rather down regulated. Unfortunately, the levels of phosphorylated PERK, eIF2α and IRE1α
450 could not be assessed due to the failure to identify specific antibodies. The decreased levels of
451 ATF4 in livers of infected animals suggests that the observed upregulation of CHOP is caused
452 by enhanced ATF6 activity. CHOP, well-known as a mediator of apoptosis, was previously
453 found to play an important role in the efficient expansion of the intracellular fungus
454 *Histoplasma capsulatum* [78]. Following infection an increase in CHOP levels led to
455 augmented apoptosis of macrophages, thus suppressing the host's defense and contributing to
456 the virulence of this particular pathogen. Another study, using intestinal epithelial cell lines,
457 showed a direct effect of heat-labile enterotoxins of *Escherichia coli* on the induction
458 upregulation of CHOP, which led to an accelerated apoptosis of the host cells [79]. Thus, the
459 upregulation of CHOP in murine hepatocytes during *E. multilocularis* infection might similarly
460 promote parasitic growth.
461 In contrast to the pro-apoptotic UPR mediator CHOP, the protein levels of the PERK target
462 ATF4 were significantly decreased in livers of *E. multilocularis* infected compared to mock-
463 infected mice. This is different from a previous study on human cutaneous leishmaniasis where
464 both CHOP and ATF4 were found to be upregulated [80]. Decreased levels of ATF4 were
465 recently described as a mechanism of acquired resistance to cope with a limited availability of
466 amino acids in cancer cells [81]. Unrestricted tumor growth requires a high demand of nutrients
467 and has been associated with a depletion of essential amino acids in the tumor tissue. Similar
468 metabolic perturbations and adaptive responses may occur in patients with hepatic AE. A recent
469 study summarizing analyses of serum samples from *E. multilocularis* infected and healthy
470 adults (group size: n=18) revealed decreased levels of branched-chain amino acids such as
471 leucine, isoleucine and valine along with lowered levels of serine and glutamine in samples
472 from infected patients [82]. In contrast, the aromatic amino acids tyrosine and phenylalanine

were increased, together with glutamate. Thus, the observed decrease in ATF4 expression may be a response to adapt the amino acid availability in the situation of parasitic growth.

Similar to ARF4 also IRE1α protein expression levels were decreased in liver tissues of AE infected mice. The reason of the decreased IRE1α expression in *E. multilocularis* infected mice and the underlying mechanism remain unclear. IRE1 enzymes are transmembrane proteins exhibiting Ser/Thr protein kinase and endoribonuclease activities and acting as major ERS sensors [83, 84]. There are two IRE1 isoforms in mammals: the ubiquitously expressed IRE1α and IRE1β which is predominantly expressed in the intestine and lung [85]. Further analysis of the liver resident IRE1α showed that the decreased protein expression in *E. multilocularis* infected mouse livers is supported by lower mRNA levels along with an increased expression of miR-1839-5p that has a target site in the 3'UTR of IRE1α as predicted by the computer-based programs Targetscan (Whitehead Institute, Cambridge, MA, USA, RRID:SCR_010845) [86] and RNA22 (Thomas Jefferson University, Philadelphia, PA, USA, RRID:SCR_016507) [87]. Additionally, miR-146a-5p was found to be enhanced in livers of infected mice. An earlier study in primary dermal fibroblasts provided evidence for a down regulation of miR-146a-5p by IRE1-dependent cleavage in response to UPR activation. A decreased hepatic IRE1α expression and activity upon *E. multilocularis* infection might suppress the activation of pro-inflammatory cytokines such as IL-1β as well as of NF-κB. Whether this promotes the progression of AE remains to be investigated.

An extensive analysis of miRs altered in livers of mice after primary infection with *E. multilocularis* by Boubaker *et al.* identified, besides miR-1839-5p and miR-146a-5p, several other miRs that were dysregulated, *i.e.* miR-148-3p, miR-15a-5p, miR-22, miR-30a-5p and miR-30a-3p [59]. The fact that miR-1839-5p and miR-146a-5p were increased in primary as well as in the secondary form of infection suggests these two miRs as potential biomarkers of AE. In this regard, Luis et al. reported an association of several circulating miRs, including miR-146a-5p, with ERS and organ damage in a model of trauma hemorrhagic shock [88].

499 Further, Wilczynski et al. reported increased miR-146a expression levels in tumor tissues of
500 patients with ovarian cancer [89]. The advanced AE resembles a tumorigenic situation with
501 alterations in the microenvironment and immune responses. Thus, follow-on research should
502 address whether miR-146a-5p and miR-1839-5p can serve as serum biomarkers of AE.
503 Beside the UPR, the ER-associated degradation (ERAD) is an important quality control
504 machinery to cope with ER stressors. ERAD plays a crucial role in the degradation of terminally
505 misfolded proteins by retro-translocating them from the ER to the cytoplasm for
506 deglycosylation and ubiquitination and subsequent proteasomal degradation [90, 91]. Prior to
507 ERAD, misfolded proteins undergo repeated cycles of re-folding by the assistance of several
508 ER-resident chaperones including lectins such as CRT and CNX, protein disulfide isomerase
509 family members like ERP72 and ERP57 as well as members of the heat shock protein 70 family
510 (e.g. GRP78) [92-95]. The elevated expression of CRT together with GRP78 and ERP72
511 indicates a higher demand for protein folding capacity in the ER in livers from infected mice.
512 This was accompanied by an elevated demand for NADPH redox equivalents in the ER and/or
513 an enhanced need for the products of the ER pentose phosphate pathway as indicated by the
514 elevated H6PD expression. H6PD was found to promote cancer cell proliferation and the
515 modulation of its expression affected GRP78, ATF6 and CHOP, emphasizing its role in ERS
516 regulation [96].
517 Importantly, treatment with the parasitostatic benzimidazole ABZ, which was shown to
518 decrease the weight of parasitic cysts in the livers of *E. multilocularis* infected mice, reversed
519 the observed effects on UPR and ERS pathways and on associated ERAD and ER redox genes.
520 In the absence of infection, ABZ did not affect any of the investigated ER related targets,
521 underlining its favorable safety profile regarding ERS related adverse effects.
522 In conclusion, the present study showed that *E. multilocularis* infection leads to a modulation
523 of the UPR, characterized by an activation of the ATF6-branch with an upregulation of CHOP
524 along with decreased ARF4 and IRE1α protein levels and increased miR-1839-5p and miR-

525 146a-5p that could serve as potential biomarkers of *E. multilocularis* infections. ABZ, the most
526 commonly used drug to treat AE ameliorated the effects of *E. multilocularis* infection on ER
527 related genes. Whether drugs targeting UPR and ERS pathways in combination with ABZ may
528 improve the treatment of AE remains to be explored.

529

530 Supplementary data

531 **S1 Table. Antibodies and corresponding dilutions.**

532 **S2 Table. Primers used for RT-qPCR.**

533 **S1 Fig. Schematic overview of experimental setup.** Animals were divided into four groups:
534 $CTRL_{(n=6)}$, $AE_{(n=6)}$, $AE\text{-}ABZ_{(n=6)}$, and $ABZ_{(n=6)}$. CTRL and ABZ mice received an
535 intraperitoneal administration of 100 µL PBS. AE and AE-ABZ mice were treated by secondary
536 *E. multilocularis* infection using approximately 100 vesicular cysts resuspended in 100 µL PBS.
537 Treatment started 6 weeks after infection. CTRL and AE mice received 100 µL corn oil orally
538 5 times per week for 8 weeks. AE-ABZ and ABZ mice received ABZ (200 mg/kg body weight)
539 in 100 µL corn oil orally 5 times per week for 8 weeks. Animals were sacrificed at the end of
540 treatment.

541 **S2 Fig. XBP1 mRNA and XBP1-s mRNA levels are not altered upon *E. multilocularis***
542 **infection.** XBP1 and XBP1-s mRNA levels in mock-infected control mice ($CTRL_{n=6}$), *E.*
543 *multilocularis* infected mice ($AE_{n=6}$), infected mice treated with ABZ ($AE\text{-}ABZ_{n=6}$) or
544 uninfected mice treated with ABZ ($ABZ_{n=6}$). Results represent mean ± SD. No outliers were
545 excluded. One-way ANOVA was applied to test significance.

546 **S3 Fig. *E. multilocularis* infection does not affect miR-15a-5p, miR-148a-3p, miR-22-3p,**
547 **miR-30a-3p and miR-30a-5p expression levels.** miR-15a-5p, miR-148a-3p, miR-22-3p, miR-
548 30a-5p and miR-30a-3p levels, in mock-infected, mock-treated mice ($CTRL_{n=6}$) and *E.*

549 *multilocularis* infected mock-treated mice (AE $_{n=6}$). Results represent mean ± SD. No outliers
550 were excluded. Two-tailed unpaired t-test was applied to test significance.

551 **S1 File. Raw data of western blots used to produce graphs and figures.**

552 **Striking image.** Experimental setup and key finding that *E. multilocularis* infection causes ER-
553 stress in mouse liver. Treatment of infected mice using the anthelminthic drug albendazole
554 attenuates the altered expression of selected ER-stress related genes.

555

556 ## Acknowledgements

557 None.

558

559 ## Data Availability

560 All relevant data are within the manuscript and in its supporting information files.

561

562 ## Author Contributions

563	***Conceptualization***	Alex Odermatt, Michael Weingartner, Fadi Jebbawi.
564	***Data curation***	Michael Weingartner, Fadi Jebbawi, Simon Stücheli
565	***Formal analysis***	Michael Weingartner, Fadi Jebbawi
566	***Funding acquisition***	Alex Odermatt, Britta Lundström-Stadelmann
567	***Investigation***	Michael Weingartner, Fadi Jebbawi, Junhua Wang
568	***Methodology***	Michael Weingartner, Fadi Jebbawi, Junhua Wang, Britta
569		Lundström-Stadelmann
570	***Project administration***	Michael Weingartner, Fadi Jebbawi
571	***Resources***	Alex Odermatt, Britta Lundström-Stadelmann, Bruno Gottstein,
572		Guido Beldi
573	***Supervision***	Alex Odermatt, Britta Lundström-Stadelmann, Bruno Gottstein,
574		Guido Beldi
575	***Visualization*:**	Michael Weingartner
576	***Writing – original draft*:**	Michael Weingartner
577	***Writing – review & editing***	All authors

Rights and permissions

References

1. Spicher M, Roethlisberger C, Lany C, Stadelmann B, Keiser J, Ortega-Mora LM, et al. In vitro and in vivo treatments of echinococcus protoscoleces and metacestodes with artemisinin and artemisinin derivatives. Antimicrob Agents Chemother. 2008;52(9):3447-50. Epub 2008/07/16. doi: 10.1128/AAC.00553-08. PubMed PMID: 18625777; PubMed Central PMCID: PMCPMC2533465.

2. Conraths FJ, Probst C, Possenti A, Boufana B, Saulle R, Torre GL, et al. Potential risk factors associated with human alveolar echinococcosis: Systematic review and meta-analysis. PLOS Neglected Tropical Diseases. 2017;11(7):e0005801. doi: 10.1371/journal.pntd.0005801.

3. Kowalczyk M, Kurpiewski W, Zieliński E, Zadrożny D, Klepacki Ł, Juśkiewicz W, et al. A rare case of the simultaneous location of Echinococcus multilocularis in the liver and the head of the pancreas: case report analysis and review of literature. BMC Infectious Diseases. 2019;19(1):661. doi: 10.1186/s12879-019-4274-y.

4. Ritler D, Rufener R, Li JV, Kämpfer U, Müller J, Bühr C, et al. In vitro metabolomic footprint of the Echinococcus multilocularis metacestode. Scientific Reports. 2019;9(1):1-13. doi: 10.1038/s41598-019-56073-y.

5. Schweiger A, Ammann RW, Candinas D, Clavien P-A, Eckert J, Gottstein B, et al. Human Alveolar Echinococcosis after Fox Population Increase, Switzerland. Emerging Infectious Diseases. 2007;13(6):878-82. doi: 10.3201/eid1306.061074.

6. Kantarci M, Bayraktutan U, Karabulut N, Aydinli B, Ogul H, Yuce I, et al. Alveolar echinococcosis: spectrum of findings at cross-sectional imaging. Radiographics.

610 2012;32(7):2053-70. Epub 2012/11/15. doi: 10.1148/rg.327125708. PubMed PMID:
611 23150858.
612 7. Kayacan SM, Vatansever S, Temiz S, Uslu B, Kayacan D, Akkaya V, et al. Alveolar
613 echinococcosis localized in the liver, lung and brain. Chin Med J (Engl). 2008;121(1):90-2.
614 Epub 2008/01/23. PubMed PMID: 18208675.
615 8. Niu F, Chong S, Qin M, Li S, Wei R, Zhao Y. Mechanism of Fibrosis Induced by
616 Echinococcus spp. Diseases. 2019;7(3). doi: 10.3390/diseases7030051.
617 9. Bulakçı M, Kartal MG, Yılmaz S, Yılmaz E, Yılmaz R, Şahin D, et al. Multimodality
618 imaging in diagnosis and management of alveolar echinococcosis: an update. Diagnostic and
619 Interventional Radiology. 2016;22(3):247-56. doi: 10.5152/dir.2015.15456.
620 10. Gottstein B, Wang J, Boubaker G, Marinova I, Spiliotis M, Muller N, et al.
621 Susceptibility versus resistance in alveolar echinococcosis (larval infection with Echinococcus
622 multilocularis). Vet Parasitol. 2015;213(3-4):103-9. Epub 2015/08/12. doi:
623 10.1016/j.vetpar.2015.07.029. PubMed PMID: 26260407.
624 11. Aasen TD, Nasrollah L, Seetharam A. Acute Liver Failure Secondary to Albendazole:
625 Defining Albendazole's Role in the Management of Echinococcal Infection: 722. American
626 Journal of Gastroenterology. 2015;110:S316.
627 12. Hemphill A, Stadelmann B, Rufener R, Spiliotis M, Boubaker G, Muller J, et al.
628 Treatment of echinococcosis: albendazole and mebendazole--what else? Parasite. 2014;21:70.
629 Epub 2014/12/20. doi: 10.1051/parasite/2014073. PubMed PMID: 25526545; PubMed
630 Central PMCID: PMCPMC4271654.
631 13. Choi GY, Yang HW, Cho SH, Kang DW, Go H, Lee WC, et al. Acute drug-induced
632 hepatitis caused by albendazole. J Korean Med Sci. 2008;23(5):903-5. Epub 2008/10/29. doi:
633 10.3346/jkms.2008.23.5.903. PubMed PMID: 18955802; PubMed Central PMCID:
634 PMCPMC2580005.
635 14. Marin Zuluaga JI, Marin Castro AE, Perez Cadavid JC, Restrepo Gutierrez JC.
636 Albendazole-induced granulomatous hepatitis: a case report. J Med Case Rep. 2013;7:201.
637 Epub 2013/07/31. doi: 10.1186/1752-1947-7-201. PubMed PMID: 23889970; PubMed
638 Central PMCID: PMCPMC3750323.
639 15. Ammann RW, Hirsbrunner R, Cotting J, Steiger U, Jacquier P, Eckert J. Recurrence
640 Rate after Discontinuation of Long-Term Mebendazole Therapy in Alveolar Echinococcosis
641 (Preliminary-Results). American Journal of Tropical Medicine and Hygiene. 1990;43(5):506-
642 15. doi: DOI 10.4269/ajtmh.1990.43.506. PubMed PMID: WOS:A1990EL12600009.

643 16. Buttenschoen K, Gruener B, Carli Buttenschoen D, Reuter S, Henne-Bruns D, Kern P.
644 Palliative operation for the treatment of alveolar echinococcosis. Langenbecks Arch Surg.
645 2009;394(1):199-204. Epub 2008/06/26. doi: 10.1007/s00423-008-0367-6. PubMed PMID:
646 18575882.
647 17. Charbonnet P, Bühler L, Sagnak E, Villiger P, Morel P, Mentha G. Devenir à long
648 terme des malades opérés et traités pour échinococcose alvéolaire. Annales de Chirurgie.
649 2004;129(6):337-42. doi: 10.1016/j.anchir.2004.01.017.
650 18. Baumann S, Shi R, Liu W, Bao H, Schmidberger J, Kratzer W, et al. Worldwide
651 literature on epidemiology of human alveolar echinococcosis: a systematic review of research
652 published in the twenty-first century. Infection. 2019;47(5):703-27. Epub 2019/05/31. doi:
653 10.1007/s15010-019-01325-2. PubMed PMID: 31147846.
654 19. Kuscher S, Kronberger IE, Loizides A, Plaikner M, Ninkovic M, Brunner A, et al.
655 Exploring the limits of hepatic surgery for alveolar echinococcosis—10-years' experience in
656 an endemic area of Austria. European Surgery. 2019;51(4):189-96. doi: 10.1007/s10353-019-
657 0596-7.
658 20. Qu B, Guo L, Sheng G, Yu F, Chen G, Wang Y, et al. Management of Advanced
659 Hepatic Alveolar Echinococcosis: Report of 42 Cases. The American Journal of Tropical
660 Medicine and Hygiene. 2017;96(3):680-5. doi: 10.4269/ajtmh.16-0557.
661 21. Sréter T, Széll Z, Egyed Z, Varga I. Echinococcus multilocularis: An Emerging
662 Pathogen in Hungary and Central Eastern Europe? Emerging Infectious Diseases.
663 2003;9(3):384-6. doi: 10.3201/eid0903.020320.
664 22. Vuitton DA, Demonmerot F, Knapp J, Richou C, Grenouillet F, Chauchet A, et al.
665 Clinical epidemiology of human AE in Europe. Veterinary Parasitology. 2015;213(3):110-20.
666 doi: 10.1016/j.vetpar.2015.07.036.
667 23. Galluzzi L, Diotallevi A, Magnani M. Endoplasmic reticulum stress and unfolded
668 protein response in infection by intracellular parasites. Future Sci OA. 2017;3(3):FSO198.
669 Epub 2017/09/09. doi: 10.4155/fsoa-2017-0020. PubMed PMID: 28883998; PubMed Central
670 PMCID: PMCPMC5583660.
671 24. Pillich H, Loose M, Zimmer KP, Chakraborty T. Diverse roles of endoplasmic
672 reticulum stress sensors in bacterial infection. Mol Cell Pediatr. 2016;3(1):9. Epub
673 2016/02/18. doi: 10.1186/s40348-016-0037-7. PubMed PMID: 26883353; PubMed Central
674 PMCID: PMCPMC4755955.

675 25. Zhang L, Wang A. Virus-induced ER stress and the unfolded protein response. Front
676 Plant Sci. 2012;3:293. Epub 2013/01/08. doi: 10.3389/fpls.2012.00293. PubMed PMID:
677 23293645; PubMed Central PMCID: PMCPMC3531707.
678 26. Neerukonda SN, Katneni UK, Bott M, Golovan SP, Parcells MS. Induction of the
679 unfolded protein response (UPR) during Marek's disease virus (MDV) infection. Virology.
680 2018;522:1-12. Epub 2018/07/07. doi: 10.1016/j.virol.2018.06.016. PubMed PMID:
681 29979959.
682 27. Mehrbod P, Ande SR, Alizadeh J, Rahimizadeh S, Shariati A, Malek H, et al. The
683 roles of apoptosis, autophagy and unfolded protein response in arbovirus, influenza virus, and
684 HIV infections. Virulence. 2019;10(SI1):376-413. doi: 10.1080/21505594.2019.1605803.
685 28. Smith JA. A new paradigm: innate immune sensing of viruses via the unfolded protein
686 response. Frontiers in Microbiology. 2014;5. doi: 10.3389/fmicb.2014.00222.
687 29. Borsa M, Ferreira PLC, Petry A, Ferreira LGE, Camargo MM, Bou-Habib DC, et al.
688 HIV infection and antiretroviral therapy lead to unfolded protein response activation. Virol J.
689 2015;12:77. doi: 10.1186/s12985-015-0298-0.
690 30. Perera N, Miller JL, Zitzmann N. The role of the unfolded protein response in dengue
691 virus pathogenesis. Cell Microbiol. 2017;19(5). doi: 10.1111/cmi.12734.
692 31. Ambrose RL, Mackenzie JM. West Nile Virus Differentially Modulates the Unfolded
693 Protein Response To Facilitate Replication and Immune Evasion. J Virol. 2011;85(6):2723-
694 32. doi: 10.1128/JVI.02050-10.
695 32. Isler JA, Skalet AH, Alwine JC. Human cytomegalovirus infection activates and
696 regulates the unfolded protein response. J Virol. 2005;79(11):6890-9. Epub 2005/05/14. doi:
697 10.1128/JVI.79.11.6890-6899.2005. PubMed PMID: 15890928; PubMed Central PMCID:
698 PMCPMC1112127.
699 33. Bechill J, Chen Z, Brewer JW, Baker SC. Coronavirus infection modulates the
700 unfolded protein response and mediates sustained translational repression. J Virol.
701 2008;82(9):4492-501. Epub 2008/02/29. doi: 10.1128/JVI.00017-08. PubMed PMID:
702 18305036; PubMed Central PMCID: PMCPMC2293058.
703 34. Burnett HF, Audas TE, Liang G, Lu RR. Herpes simplex virus-1 disarms the unfolded
704 protein response in the early stages of infection. Cell Stress Chaperones. 2012;17(4):473-83.
705 Epub 2012/01/25. doi: 10.1007/s12192-012-0324-8. PubMed PMID: 22270612; PubMed
706 Central PMCID: PMCPMC3368031.
707 35. Ii Timberlake M, Dwivedi Y. Linking unfolded protein response to inflammation and
708 depression: potential pathologic and therapeutic implications. Mol Psychiatry.

2019;24(7):987-94. Epub 2018/09/15. doi: 10.1038/s41380-018-0241-z. PubMed PMID: 30214045; PubMed Central PMCID: PMCPMC6416085.

36. So JS. Roles of Endoplasmic Reticulum Stress in Immune Responses. Mol Cells. 2018;41(8):705-16. Epub 2018/08/07. doi: 10.14348/molcells.2018.0241. PubMed PMID: 30078231; PubMed Central PMCID: PMCPMC6125421.

37. Treacy-Abarca S, Mukherjee S. Legionella suppresses the host unfolded protein response via multiple mechanisms. Nature Communications. 2015;6. doi: 10.1038/ncomms8887.

38. Lim YJ, Choi JA, Choi HH, Cho SN, Kim HJ, Jo EK, et al. Endoplasmic reticulum stress pathway-mediated apoptosis in macrophages contributes to the survival of Mycobacterium tuberculosis. PLoS One. 2011;6(12):e28531. Epub 2011/12/24. doi: 10.1371/journal.pone.0028531. PubMed PMID: 22194844; PubMed Central PMCID: PMCPMC3237454.

39. Wang T, Zhou J, Gan X, Wang H, Ding X, Chen L, et al. Toxoplasma gondii induce apoptosis of neural stem cells via endoplasmic reticulum stress pathway. Parasitology. 2014;141(7):988-95. doi: 10.1017/S0031182014000183.

40. Inácio P, Zuzarte-Luís V, Ruivo MTG, Falkard B, Nagaraj N, Rooijers K, et al. Parasite-induced ER stress response in hepatocytes facilitates Plasmodium liver stage infection. EMBO reports. 2015;16(8):955-64. doi: 10.15252/embr.201439979.

41. Banerjee A, Czinn SJ, Reiter RJ, Blanchard TG. Crosstalk between endoplasmic reticulum stress and anti-viral activities: A novel therapeutic target for COVID-19. Life Sciences. 2020;255:117842. doi: 10.1016/j.lfs.2020.117842.

42. Crunkhorn S. ER stress modulator reverses diabetes. Nature Reviews Drug Discovery. 2015;14(8):528-. doi: 10.1038/nrd4702.

43. Schögler A, Caliaro O, Brügger M, Oliveira Esteves BI, Nita I, Gazdhar A, et al. Modulation of the unfolded protein response pathway as an antiviral approach in airway epithelial cells. Antiviral Research. 2019;162:44-50. doi: 10.1016/j.antiviral.2018.12.007.

44. Leung AK, Calabrese JM, Sharp PA. Quantitative analysis of Argonaute protein reveals microRNA-dependent localization to stress granules. Proc Natl Acad Sci U S A. 2006;103(48):18125-30. Epub 2006/11/23. doi: 10.1073/pnas.0608845103. PubMed PMID: 17116888; PubMed Central PMCID: PMCPMC1838717.

45. Leung AK, Sharp PA. Function and localization of microRNAs in mammalian cells. Cold Spring Harb Symp Quant Biol. 2006;71:29-38. Epub 2007/03/27. doi: 10.1101/sqb.2006.71.049. PubMed PMID: 17381277.

743 46. Geslain R, Cubells L, Bori-Sanz T, Alvarez-Medina R, Rossell D, Marti E, et al.
744 Chimeric tRNAs as tools to induce proteome damage and identify components of stress
745 responses. Nucleic Acids Res. 2010;38(5):e30. Epub 2009/12/17. doi: 10.1093/nar/gkp1083.
746 PubMed PMID: 20007146; PubMed Central PMCID: PMCPMC2836549.
747 47. Maurel M, Chevet E. Endoplasmic reticulum stress signaling: the microRNA
748 connection. Am J Physiol Cell Physiol. 2013;304(12):C1117-26. Epub 2013/03/22. doi:
749 10.1152/ajpcell.00061.2013. PubMed PMID: 23515532.
750 48. Zhou X, Li X, Wu M. miRNAs reshape immunity and inflammatory responses in
751 bacterial infection. Signal Transduct Target Ther. 2018;3:14. Epub 2018/05/31. doi:
752 10.1038/s41392-018-0006-9. PubMed PMID: 29844933; PubMed Central PMCID:
753 PMCPMC5968033.
754 49. Drury RE, O'Connor D, Pollard AJ. The Clinical Application of MicroRNAs in
755 Infectious Disease. Front Immunol. 2017;8:1182. Epub 2017/10/11. doi:
756 10.3389/fimmu.2017.01182. PubMed PMID: 28993774; PubMed Central PMCID:
757 PMCPMC5622146.
758 50. Tribolet L, Kerr E, Cowled C, Bean AGD, Stewart CR, Dearnley M, et al. MicroRNA
759 Biomarkers for Infectious Diseases: From Basic Research to Biosensing. Front Microbiol.
760 2020;11:1197. Epub 2020/06/26. doi: 10.3389/fmicb.2020.01197. PubMed PMID: 32582115;
761 PubMed Central PMCID: PMCPMC7286131.
762 51. Gallo A, Tandon M, Alevizos I, Illei GG. The majority of microRNAs detectable in
763 serum and saliva is concentrated in exosomes. PLoS One. 2012;7(3):e30679. Epub
764 2012/03/20. doi: 10.1371/journal.pone.0030679. PubMed PMID: 22427800; PubMed Central
765 PMCID: PMCPMC3302865.
766 52. Wu L, Zheng K, Yan C, Pan X, Liu Y, Liu J, et al. Genome-wide study of salivary
767 microRNAs as potential noninvasive biomarkers for detection of nasopharyngeal carcinoma.
768 BMC Cancer. 2019;19(1):843. Epub 2019/08/29. doi: 10.1186/s12885-019-6037-y. PubMed
769 PMID: 31455274; PubMed Central PMCID: PMCPMC6712819.
770 53. Ishige F, Hoshino I, Iwatate Y, Chiba S, Arimitsu H, Yanagibashi H, et al. MIR1246
771 in body fluids as a biomarker for pancreatic cancer. Sci Rep. 2020;10(1):8723. Epub
772 2020/05/28. doi: 10.1038/s41598-020-65695-6. PubMed PMID: 32457495; PubMed Central
773 PMCID: PMCPMC7250935.
774 54. Sisto R, Capone P, Cerini L, Sanjust F, Paci E, Pigini D, et al. Circulating microRNAs
775 as potential biomarkers of occupational exposure to low dose organic solvents. Toxicol Rep.

776 2019;6:126-35. Epub 2019/01/24. doi: 10.1016/j.toxrep.2019.01.001. PubMed PMID:
777 30671348; PubMed Central PMCID: PMCPMC6330509.
778 55. Byrd AE, Brewer JW. Micro(RNA)managing endoplasmic reticulum stress. IUBMB
779 Life. 2013;65(5):373-81. Epub 2013/04/05. doi: 10.1002/iub.1151. PubMed PMID:
780 23554021; PubMed Central PMCID: PMCPMC3637854.
781 56. Bartoszewska S, Kochan K, Madanecki P, Piotrowski A, Ochocka R, Collawn JF, et
782 al. Regulation of the unfolded protein response by microRNAs. Cell Mol Biol Lett.
783 2013;18(4):555-78. Epub 2013/10/05. doi: 10.2478/s11658-013-0106-z. PubMed PMID:
784 24092331; PubMed Central PMCID: PMCPMC3877167.
785 57. Lerner AG, Upton JP, Praveen PV, Ghosh R, Nakagawa Y, Igbaria A, et al. IRE1alpha
786 induces thioredoxin-interacting protein to activate the NLRP3 inflammasome and promote
787 programmed cell death under irremediable ER stress. Cell Metab. 2012;16(2):250-64. Epub
788 2012/08/14. doi: 10.1016/j.cmet.2012.07.007. PubMed PMID: 22883233; PubMed Central
789 PMCID: PMCPMC4014071.
790 58. Upton JP, Wang L, Han D, Wang ES, Huskey NE, Lim L, et al. IRE1alpha cleaves
791 select microRNAs during ER stress to derepress translation of proapoptotic Caspase-2.
792 Science. 2012;338(6108):818-22. Epub 2012/10/09. doi: 10.1126/science.1226191. PubMed
793 PMID: 23042294; PubMed Central PMCID: PMCPMC3742121.
794 59. Boubaker G, Strempel S, Hemphill A, Muller N, Wang J, Gottstein B, et al.
795 Regulation of hepatic microRNAs in response to early stage Echinococcus multilocularis egg
796 infection in C57BL/6 mice. PLoS Negl Trop Dis. 2020;14(5):e0007640. Epub 2020/05/23.
797 doi: 10.1371/journal.pntd.0007640. PubMed PMID: 32442168; PubMed Central PMCID:
798 PMCPMC7244097 following competing interests: Sebastian Strempel is employee of
799 Microsynth AG.
800 60. F J. Innate and adaptive immune responses following PD-L1 immune checkpoint
801 blockade in treating chronic alveolar echinococcosis. N/A. 2020;N/A.
802 61. Wang J, Jebbawi F, Bellanger A-P, Beldi G, Millon L, Gottstein B. Immunotherapy of
803 alveolar echinococcosis via PD-1/PD-L1 immune checkpoint blockade in mice. Parasite
804 Immunology. 2018;40(12):e12596. doi: 10.1111/pim.12596.
805 62. Weingartner M, Stücheli S. The ratio of ursodeoxycholyltaurine to 7-
806 oxolithocholyltaurine serves as a biomarker of decreased 11β-hydroxysteroid dehydrogenase
807 1 activity in mouse.

808 63. Schmittgen TD, Livak KJ. Analyzing real-time PCR data by the comparative C(T)
809 method. Nat Protoc. 2008;3(6):1101-8. Epub 2008/06/13. doi: 10.1038/nprot.2008.73.
810 PubMed PMID: 18546601.
811 64. Celli J, Tsolis RM. Bacteria, the endoplasmic reticulum and the unfolded protein
812 response: friends or foes? Nat Rev Microbiol. 2015;13(2):71-82. Epub 2014/12/24. doi:
813 10.1038/nrmicro3393. PubMed PMID: 25534809; PubMed Central PMCID:
814 PMCPMC4447104.
815 65. Pathinayake PS, Hsu ACY, Waters DW, Hansbro PM, Wood LG, Wark PAB.
816 Understanding the Unfolded Protein Response in the Pathogenesis of Asthma. Frontiers in
817 Immunology. 2018;9. doi: 10.3389/fimmu.2018.00175.
818 66. Abhishek K, Das S, Kumar A, Kumar A, Kumar V, Saini S, et al. Leishmania
819 donovani induced Unfolded Protein Response delays host cell apoptosis in PERK dependent
820 manner. PLoS Neglected Tropical Diseases. 2018;12(7). doi: 10.1371/journal.pntd.0006646.
821 67. Adams CJ, Kopp MC, Larburu N, Nowak PR, Ali MMU. Structure and Molecular
822 Mechanism of ER Stress Signaling by the Unfolded Protein Response Signal Activator IRE1.
823 Frontiers in Molecular Biosciences. 2019;6. doi: 10.3389/fmolb.2019.00011.
824 68. Amen OM, Sarker SD, Ghildyal R, Arya A. Endoplasmic Reticulum Stress Activates
825 Unfolded Protein Response Signaling and Mediates Inflammation, Obesity, and Cardiac
826 Dysfunction: Therapeutic and Molecular Approach. Frontiers in Pharmacology. 2019;10. doi:
827 10.3389/fphar.2019.00977.
828 69. Bergmann TJ, Molinari M. Three branches to rule them all? UPR signalling in
829 response to chemically versus misfolded proteins-induced ER stress. Biology of the Cell.
830 2018;110(9):197-204. doi: 10.1111/boc.201800029.
831 70. Bravo R, Parra V, Gatica D, Rodriguez AE, Torrealba N, Paredes F, et al.
832 Endoplasmic reticulum and the unfolded protein response: dynamics and metabolic
833 integration. Int Rev Cell Mol Biol. 2013;301:215-90. Epub 2013/01/16. doi: 10.1016/B978-0-
834 12-407704-1.00005-1. PubMed PMID: 23317820; PubMed Central PMCID:
835 PMCPMC3666557.
836 71. Hollien J. Evolution of the unfolded protein response. Biochimica et Biophysica Acta
837 (BBA) - Molecular Cell Research. 2013;1833(11):2458-63. doi:
838 10.1016/j.bbamcr.2013.01.016.
839 72. Clark EM, Nonarath HJT, Bostrom JR, Link BA. Establishment and validation of an
840 endoplasmic reticulum stress reporter to monitor zebrafish ATF6 activity in development and
841 disease. Disease Models & Mechanisms. 2020;13(1). doi: 10.1242/dmm.041426.

842 73. Oslowski CM, Urano F. Measuring ER stress and the unfolded protein response using
843 mammalian tissue culture system. Methods in enzymology. 2011;490:71-92. doi:
844 10.1016/B978-0-12-385114-7.00004-0.
845 74. Sundaram A, Appathurai S, Plumb R, Mariappan M. Dynamic changes in complexes
846 of IRE1α, PERK, and ATF6α during endoplasmic reticulum stress. Molecular Biology of the
847 Cell. 2018;29(11):1376-88. doi: 10.1091/mbc.E17-10-0594.
848 75. Walter P, Ron D. The Unfolded Protein Response: From Stress Pathway to
849 Homeostatic Regulation. Science. 2011;334(6059):1081-6. doi: 10.1126/science.1209038.
850 76. Shaheen A. Effect of the unfolded protein response on ER protein export: a potential
851 new mechanism to relieve ER stress. Cell Stress & Chaperones. 2018;23(5):797-806. doi:
852 10.1007/s12192-018-0905-2.
853 77. Almanza A, Carlesso A, Chintha C, Creedican S, Doultsinos D, Leuzzi B, et al.
854 Endoplasmic reticulum stress signalling – from basic mechanisms to clinical applications. The
855 FEBS Journal. 2019;286(2):241-78. doi: 10.1111/febs.14608.
856 78. English BC, Van Prooyen N, Ord T, Ord T, Sil A. The transcription factor CHOP, an
857 effector of the integrated stress response, is required for host sensitivity to the fungal
858 intracellular pathogen Histoplasma capsulatum. PLoS Pathog. 2017;13(9):e1006589. Epub
859 2017/09/28. doi: 10.1371/journal.ppat.1006589. PubMed PMID: 28953979; PubMed Central
860 PMCID: PMCPMC5633207.
861 79. Lu X, Li C, Li C, Li P, Fu E, Xie Y, et al. Heat-Labile Enterotoxin-Induced PERK-
862 CHOP Pathway Activation Causes Intestinal Epithelial Cell Apoptosis. Front Cell Infect
863 Microbiol. 2017;7:244. Epub 2017/06/24. doi: 10.3389/fcimb.2017.00244. PubMed PMID:
864 28642847; PubMed Central PMCID: PMCPMC5463185.
865 80. Dias-Teixeira KL, Calegari-Silva TC, Medina JM, Vivarini AC, Cavalcanti A, Teteo
866 N, et al. Emerging Role for the PERK/eIF2alpha/ATF4 in Human Cutaneous Leishmaniasis.
867 Sci Rep. 2017;7(1):17074. Epub 2017/12/08. doi: 10.1038/s41598-017-17252-x. PubMed
868 PMID: 29213084; PubMed Central PMCID: PMCPMC5719050.
869 81. Mesclon F, Lambert-Langlais S, Carraro V, Parry L, Hainault I, Jousse C, et al.
870 Decreased ATF4 expression as a mechanism of acquired resistance to long-term amino acid
871 limitation in cancer cells. Oncotarget. 2017;8(16):27440-53. Epub 2017/05/04. doi:
872 10.18632/oncotarget.15828. PubMed PMID: 28460466; PubMed Central PMCID:
873 PMCPMC5432347.
874 82. Lin C, Chen Z, Zhang L, Wei Z, Cheng KK, Liu Y, et al. Deciphering the metabolic
875 perturbation in hepatic alveolar echinococcosis: a (1)H NMR-based metabolomics study.

876 Parasit Vectors. 2019;12(1):300. Epub 2019/06/15. doi: 10.1186/s13071-019-3554-0.
877 PubMed PMID: 31196218; PubMed Central PMCID: PMCPMC6567409.
878 83. Paschen W, Mengesdorf T. Endoplasmic reticulum stress response and
879 neurodegeneration. Cell Calcium. 2005;38(3-4):409-15. Epub 2005/08/10. doi:
880 10.1016/j.ceca.2005.06.019. PubMed PMID: 16087231.
881 84. Chen Y, Brandizzi F. IRE1: ER stress sensor and cell fate executor. Trends Cell Biol.
882 2013;23(11):547-55. Epub 2013/07/25. doi: 10.1016/j.tcb.2013.06.005. PubMed PMID:
883 23880584; PubMed Central PMCID: PMCPMC3818365.
884 85. Akhter MS, Uddin MA, Kubra KT, Barabutis N. Autophagy, Unfolded Protein
885 Response and Lung Disease. Curr Res Cell Biol. 2020;1. Epub 2020/11/10. doi:
886 10.1016/j.crcbio.2020.100003. PubMed PMID: 33163960; PubMed Central PMCID:
887 PMCPMC7643908.
888 86. Agarwal V, Bell GW, Nam JW, Bartel DP. Predicting effective microRNA target sites
889 in mammalian mRNAs. Elife. 2015;4. Epub 2015/08/13. doi: 10.7554/eLife.05005. PubMed
890 PMID: 26267216; PubMed Central PMCID: PMCPMC4532895.
891 87. Miranda KC, Huynh T, Tay Y, Ang YS, Tam WL, Thomson AM, et al. A pattern-
892 based method for the identification of MicroRNA binding sites and their corresponding
893 heteroduplexes. Cell. 2006;126(6):1203-17. Epub 2006/09/23. doi:
894 10.1016/j.cell.2006.07.031. PubMed PMID: 16990141.
895 88. Luis A, Hackl M, Jafarmadar M, Keibl C, Jilge JM, Grillari J, et al. Circulating
896 miRNAs Associated With ER Stress and Organ Damage in a Preclinical Model of Trauma
897 Hemorrhagic Shock. Front Med (Lausanne). 2020;7:568096. Epub 2020/10/20. doi:
898 10.3389/fmed.2020.568096. PubMed PMID: 33072784; PubMed Central PMCID:
899 PMCPMC7542230.
900 89. Wilczynski M, Zytko E, Szymanska B, Dzieniecka M, Nowak M, Danielska J, et al.
901 Expression of miR-146a in patients with ovarian cancer and its clinical significance. Oncol
902 Lett. 2017;14(3):3207-14. Epub 2017/09/21. doi: 10.3892/ol.2017.6477. PubMed PMID:
903 28927067; PubMed Central PMCID: PMCPMC5588008.
904 90. Halperin L, Jung J, Michalak M. The many functions of the endoplasmic reticulum
905 chaperones and folding enzymes. IUBMB Life. 2014;66(5):318-26. doi: 10.1002/iub.1272.
906 91. Ruggiano A, Foresti O, Carvalho P. ER-associated degradation: Protein quality control
907 and beyond. Journal of Cell Biology. 2014;204(6):869-79. doi: 10.1083/jcb.201312042.

908 92. Danilczyk UG, Cohen-Doyle MF, Williams DB. Functional Relationship between
909 Calreticulin, Calnexin, and the Endoplasmic Reticulum Luminal Domain of Calnexin. Journal
910 of Biological Chemistry. 2000;275(17):13089-97. doi: 10.1074/jbc.275.17.13089.
911 93. Ni M, Lee AS. ER chaperones in mammalian development and human diseases. FEBS
912 letters. 2007;581(19):3641-51. doi: 10.1016/j.febslet.2007.04.045.
913 94. Radons J. The human HSP70 family of chaperones: where do we stand? Cell Stress &
914 Chaperones. 2016;21(3):379-404. doi: 10.1007/s12192-016-0676-6.
915 95. Williams DB. Beyond lectins: the calnexin/calreticulin chaperone system of the
916 endoplasmic reticulum. Journal of Cell Science. 2006;119(4):615-23. doi: 10.1242/jcs.02856.
917 96. Tsachaki M, Mladenovic N, Stambergova H, Birk J, Odermatt A. Hexose-6-phosphate
918 dehydrogenase controls cancer cell proliferation and migration through pleiotropic effects on
919 the unfolded-protein response, calcium homeostasis, and redox balance. FASEB J.
920 2018;32(5):2690-705. Epub 2018/01/04. doi: 10.1096/fj.201700870RR. PubMed PMID:
921 29295867; PubMed Central PMCID: PMCPMC5901385.

922

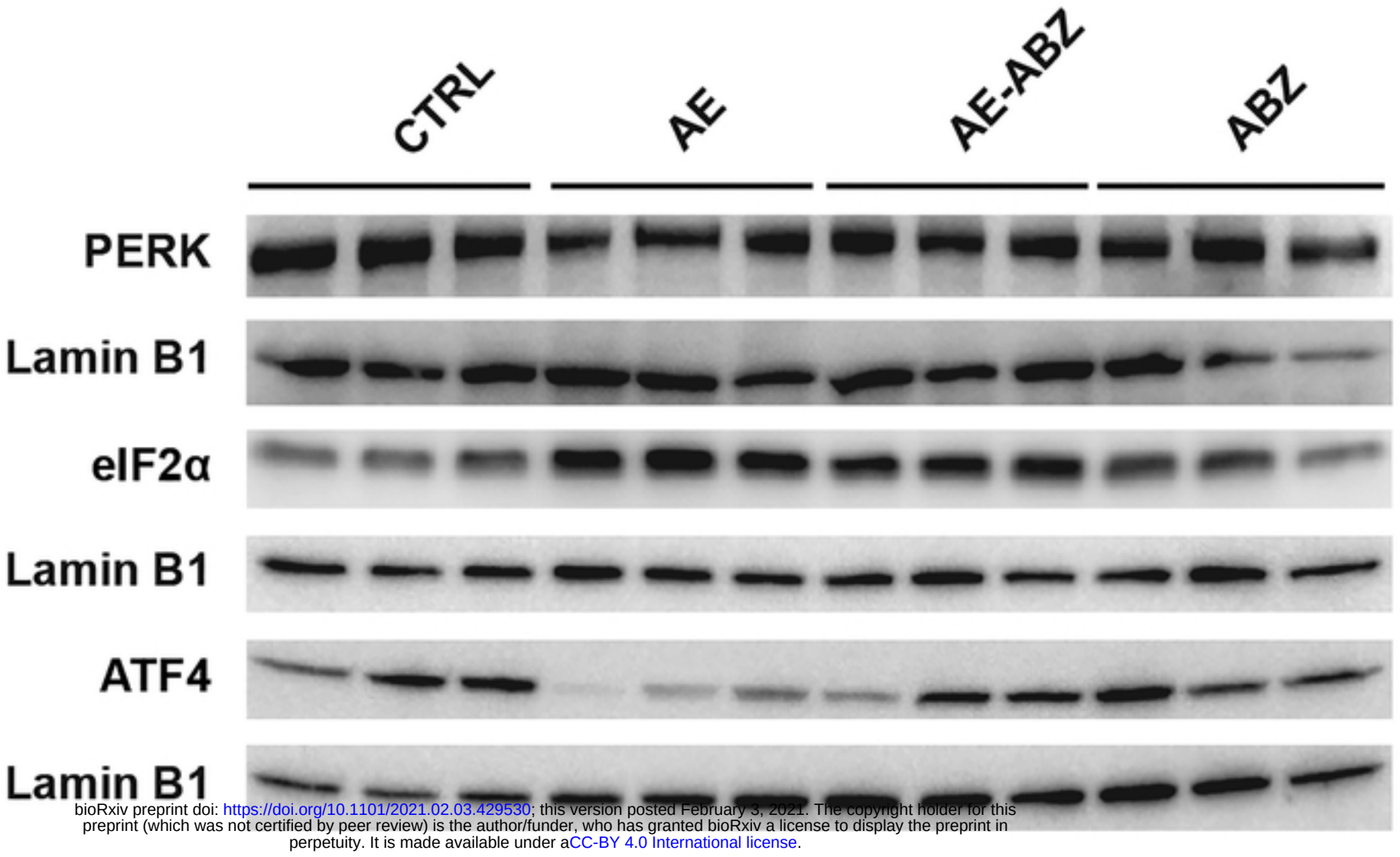

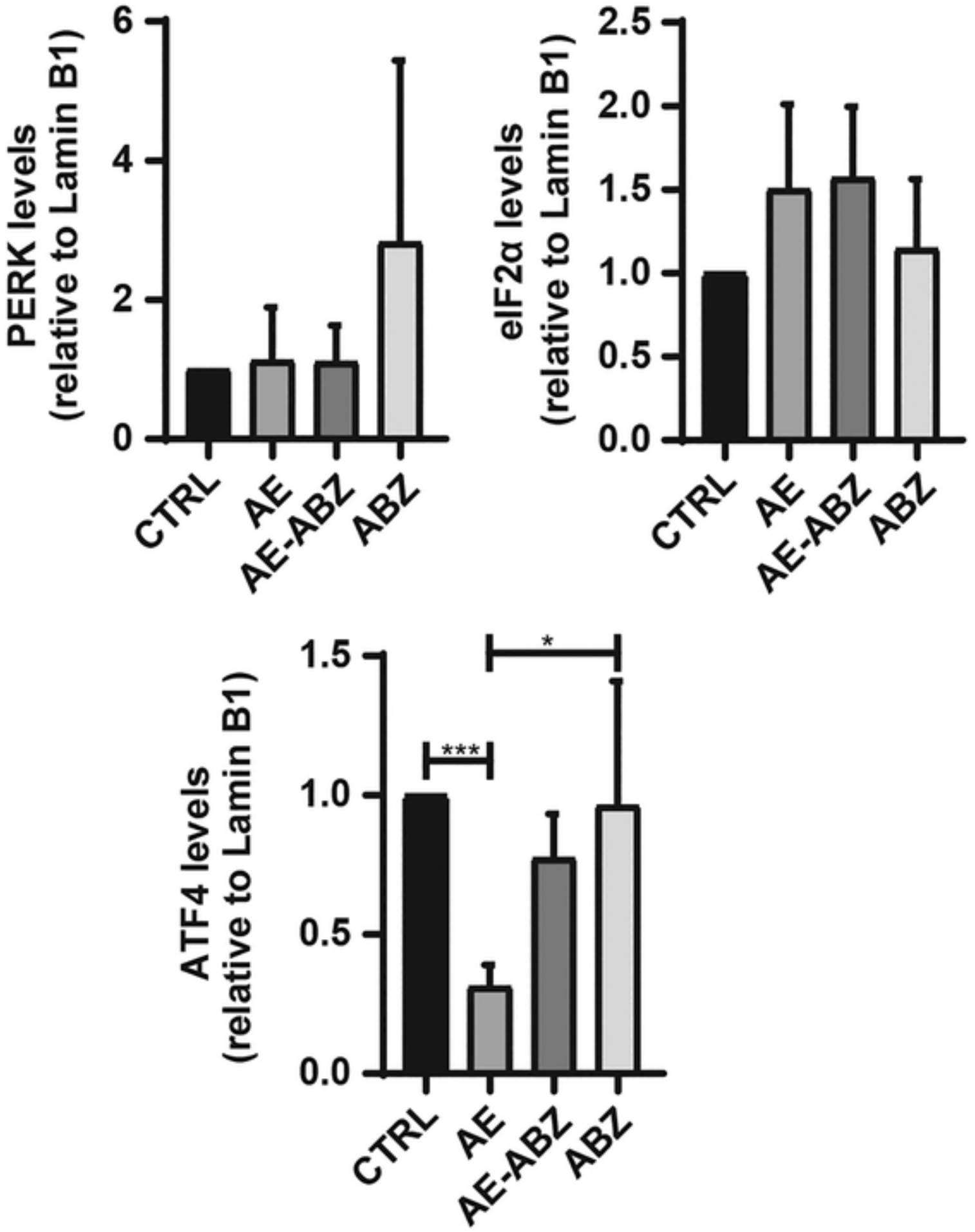

Figure1

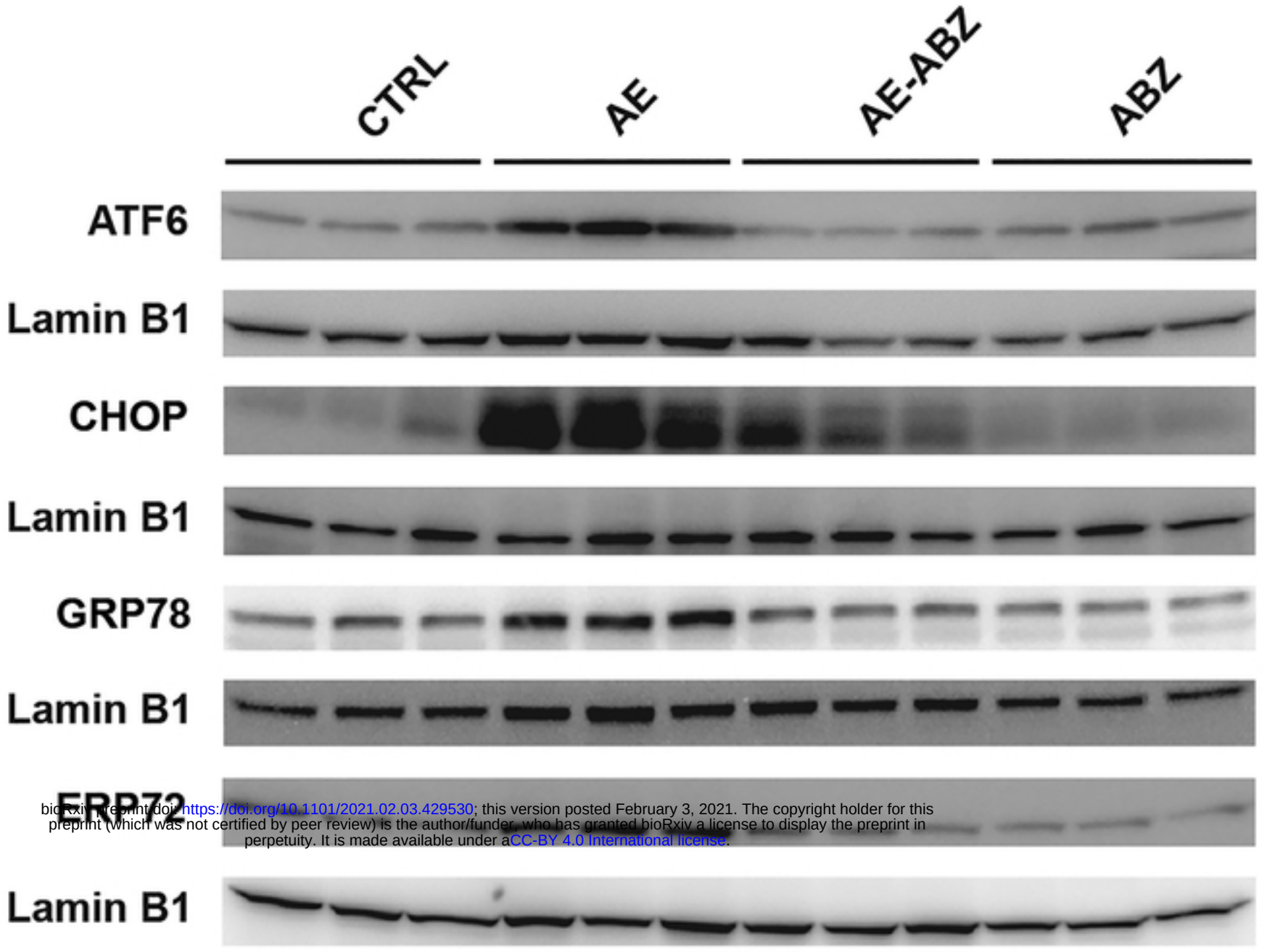

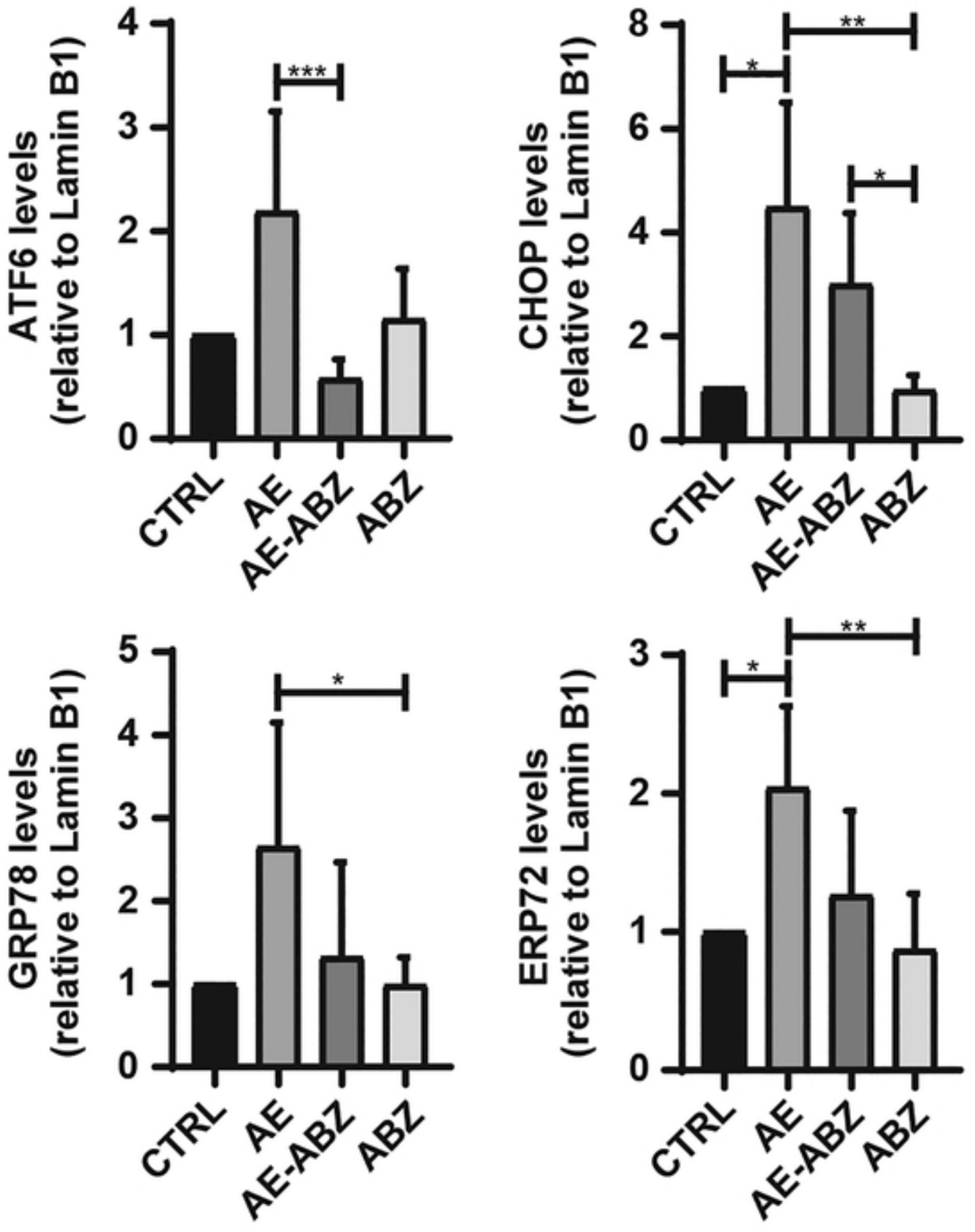

Figure2

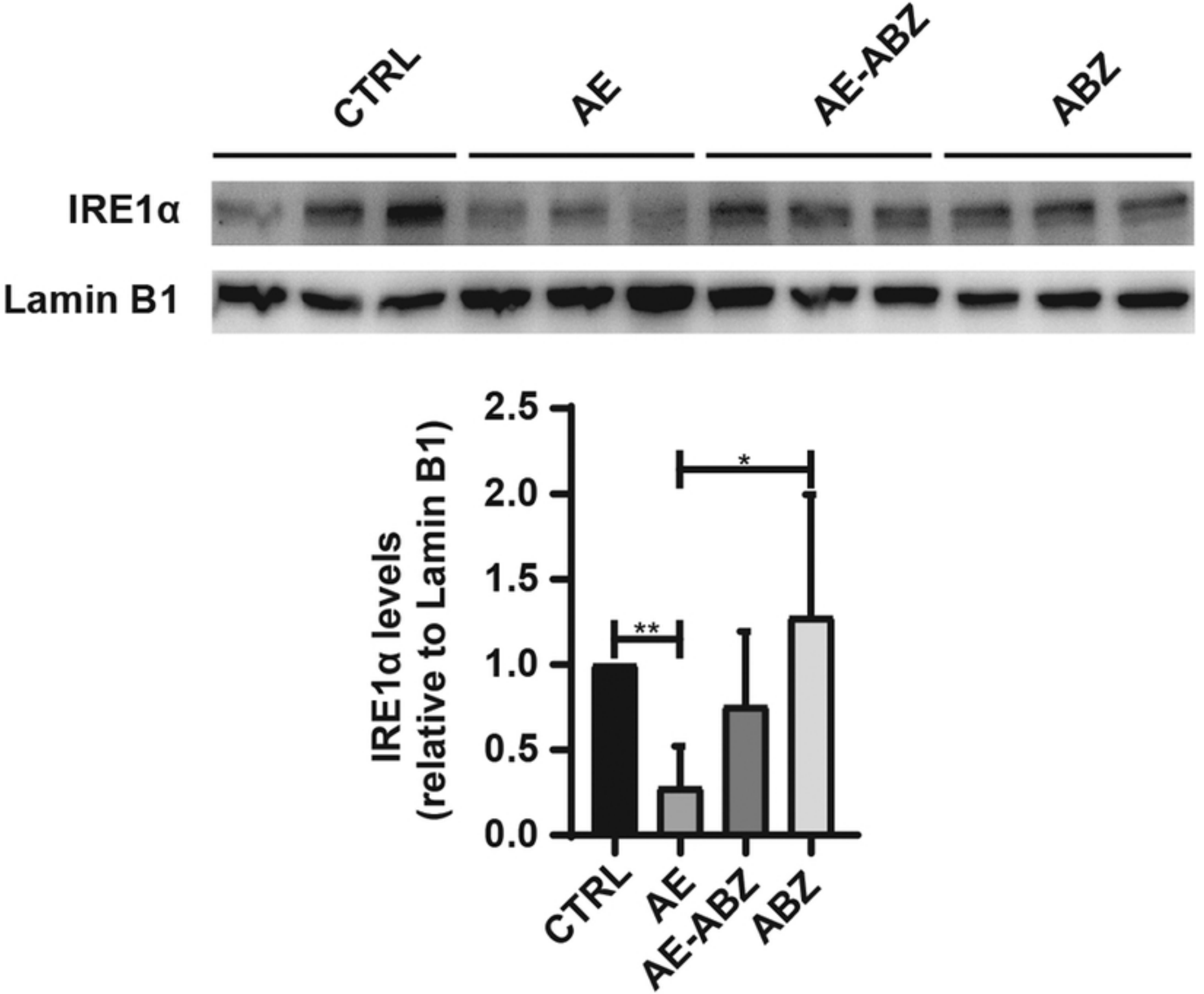
CTRL
AE
AE-ABZ
ABZ
IRE1α
Lamin B1
IRE1α levels
(relative to Lamin B1)
2.5
2.0
1.5
1.0
0.5
0.0
*
**
CTRL
AE
AE-ABZ
ABZ

Figure3

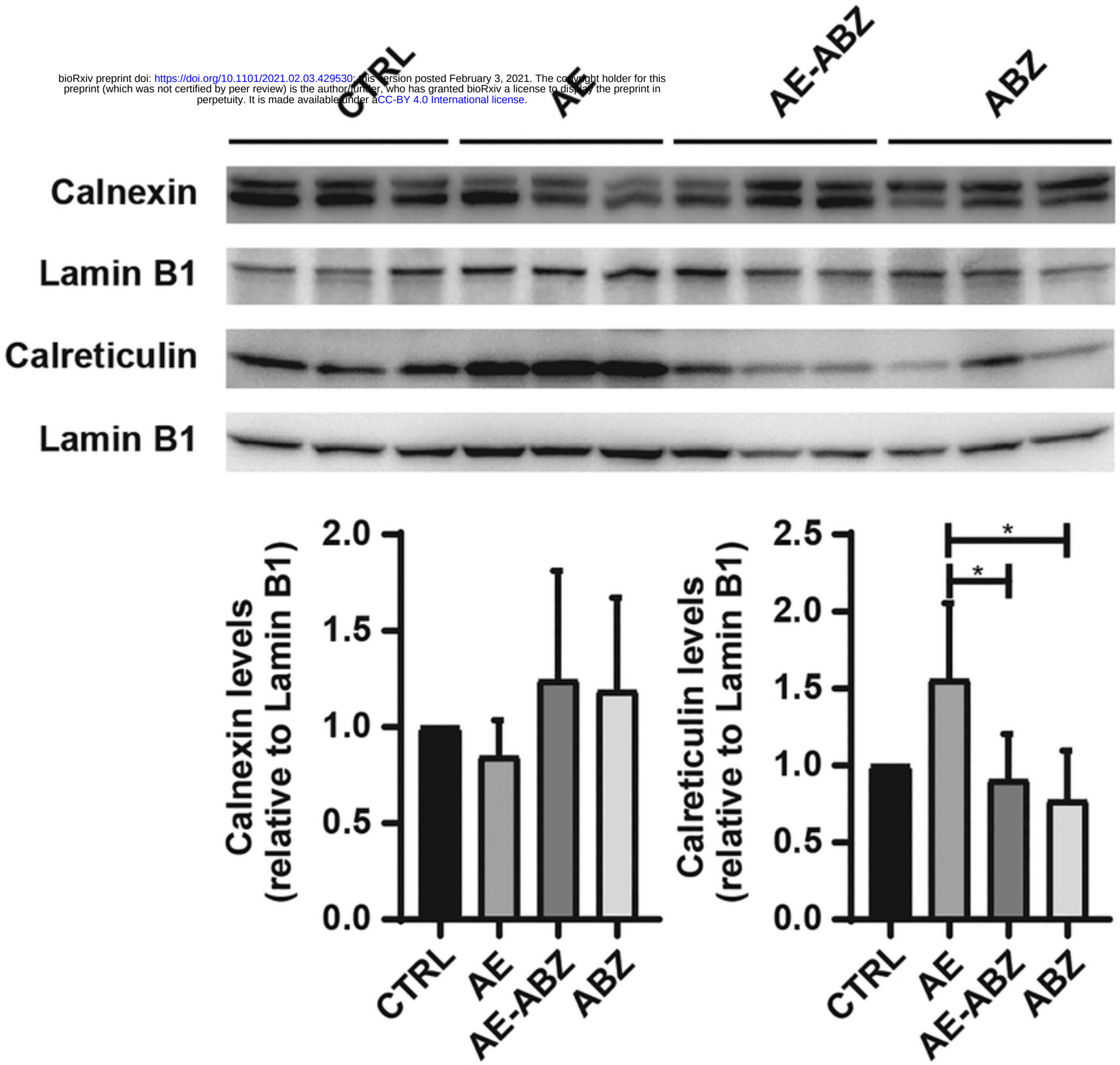

Figure4

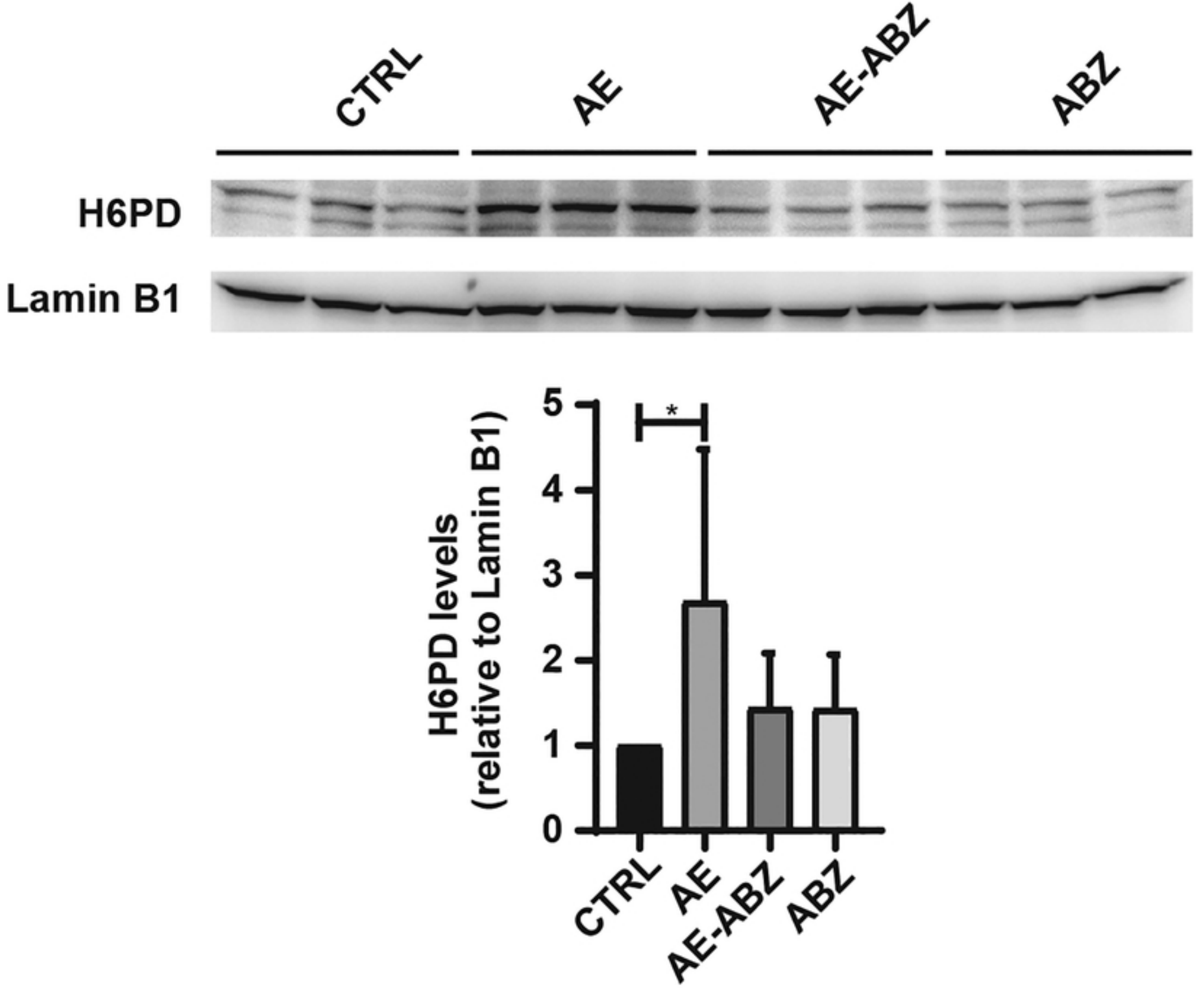
CTRL
AE
AE-ABZ
ABZ
H6PD
Lamin B1
H6PD levels
(relative to Lamin B1)
5
4
3
2
1
0
*
CTRL
AE
AE-ABZ
ABZ

Figure5

A

IRE1α - Mus Musculus

```
                                                    5′UTR
   1 gcccgccccg accggaagaa gccgggacac aaggcactta tagggctggg aatgggggtg
  //                                                CDS
1381 agcctgaggc ccccgtggac tccatgctca aggacatggc taccattatc ctgagcacct
1441 tcctgctggt tggatgggtg gcgttcatca tcacttaccc cctgagcgtg catcagcagc
  //                                                3′UTR
3001 catatgccct ctgagctagg gcagccctct ggtctggtgg ccccaataat gaccatgggc
3061 ccgatctctg cagtcatagt ttgttgcctc tgggattagc aggaagacta agcttcgcaa
                                                    miR-1839-5p
 //                                                  ga -tggaa
                                                     ||  |||||
4681 atgtgaggaa gaggaaccaa tgtcaccggg ggctgctgct cacctt gctc ctcgtgcctg
 //
6841 attctgctca ttgatgaagg cgacttatgc tgagccaacc acaaataaag gtagttttag
6901 atttggga
 //
```

B

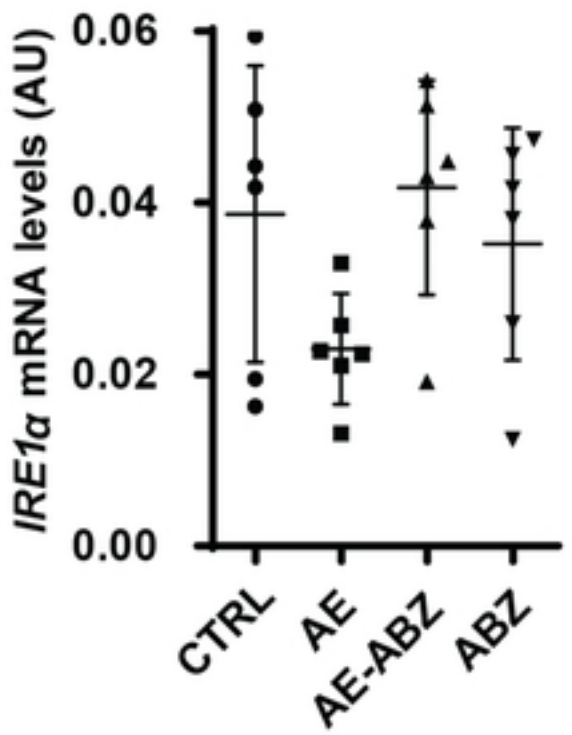

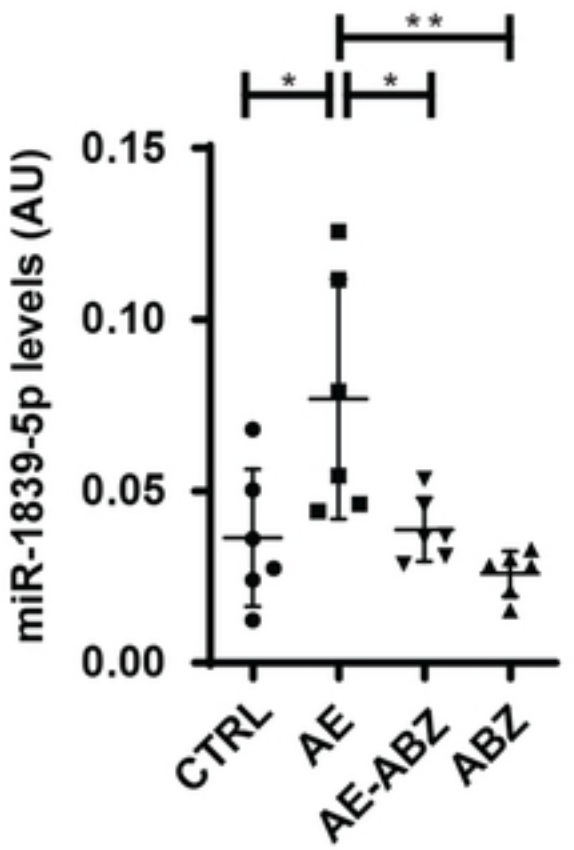

C

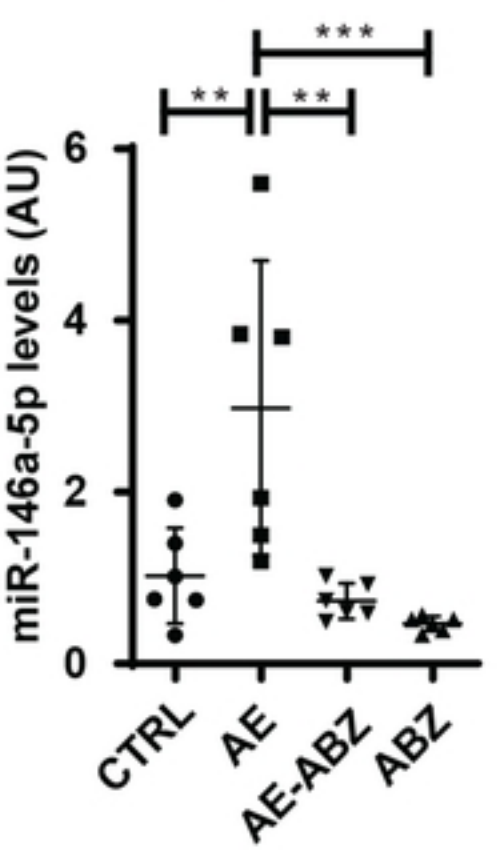

Figure6

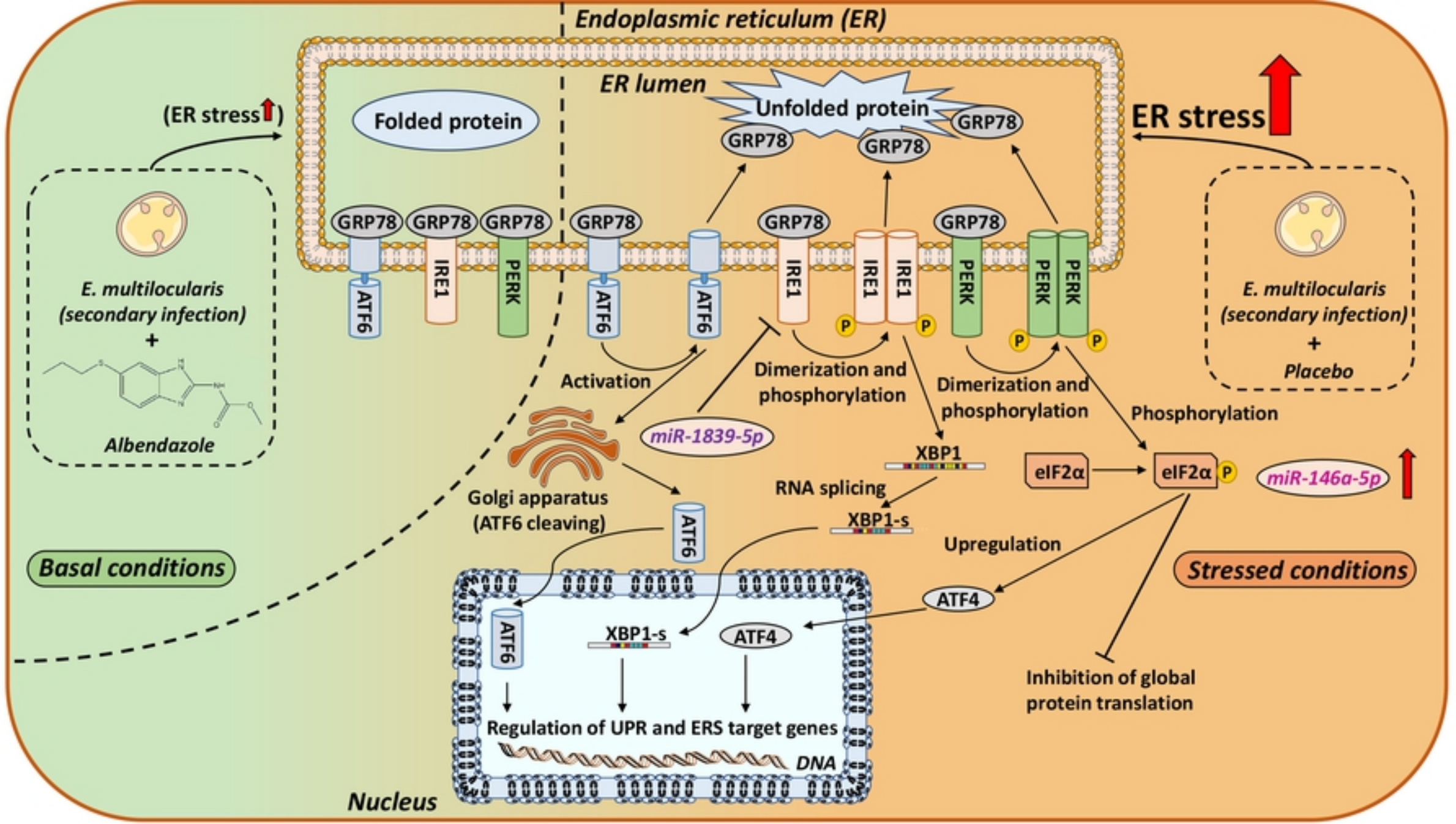
Endoplasmic reticulum (ER)
ER lumen
Folded protein
Unfolded protein
GRP78
(ER stress)
ER stress
E. multilocularis
(secondary infection)
+
Albendazole
E. multilocularis
(secondary infection)
+
Placebo
ATF6
IRE1
PERK
P
Activation
Dimerization and
phosphorylation
Dimerization and
phosphorylation
Phosphorylation
miR-1839-5p
XBP1
RNA splicing
XBP1-s
eIF2α
miR-146a-5p
Golgi apparatus
(ATF6 cleaving)
Basal conditions
Stressed conditions
Upregulation
ATF4
Inhibition of global
protein translation
Regulation of UPR and ERS target genes
DNA
Nucleus

Figure7